molecular arms to sensitively detect viral RNA. The molecular complexes sensing viral RNA may not be so simple that we will be able to identify more molecules than Riplet as enhancers for integral RNA recognition. In either case, yeast screening will be a good strategy to pick up such proteins in other RNA recognition systems. A molecular switch selecting IFN induction by virus RNA will then be clarified.

We show that the ubiquitination sites targeted by Riplet are the helicase and RD domains of RIG-I but not its CARD-like domains in contrast to TRIM25. Riplet may be a complement factor of the reported TRIM25 function for RIG-I activation (23). A previous report (25) failed to polyubiquitinate the RIG-I protein by TRIM25 alone. If Riplet were added to TRIM25 for RIG-I ubiquitination in the previous study, Riplet would have enabled TRIM25 to polyubiquitinate the RIG-I CARD-like region. Further studies using TRIM25 and Riplet will be required to clarify this point.

Based on our results, we propose that RIG-I-like receptors form a molecular complex that efficiently recognizes low copy numbers of viral RNA. Riplet is implicated in the RIG-I complex to enhance viral RNA response in some organs. In this context, MDA5-associated molecules might also exist in the cytoplasm to augment IFN output. Although MDA5 possesses the RD domain, it fails to recruit Riplet (data not shown) or augment IFN-β-induction in conjunction with Riplet (Fig. 2*E*). Because RLR-associated molecules naturally reside in cells and facilitate inhibition of low dose viral infection until RLRs become expressed, they may be useful therapeutic targets for an early phase antiviral immunotherapy.

Acknowledgments—We thank Dr. M. Sasai in our laboratory for technical instructions for assay of RIG-I functions and Drs. K. Shimotohno (Keio University), T. Taniguchi (University of Tokyo), and T. Fujita (Kyoto University) for their critical discussions.

REFERENCES

1. Takeuchi, O., and Akira, S. (2008) *Curr. Opin. Immunol.* **20,** 17–22
2. Honda, K., Takaoka, A., and Taniguchi, T. (2006) *Immunity* **25,** 349–360
3. Kato, H., Takeuchi, O., Sato, S., Yoneyama, M., Yamamoto, M., Matsui, K., Uematsu, S., Jung, A., Kawai, T., Ishii, K. J., Yamaguchi, O., Otsu, K., Tsujimura, T., Koh, C. S., Reis e Sousa, C., Matsuura, Y., Fujita, T., and Akira, S. (2006) *Nature* **441,** 101–105
4. Venkataraman, T., Valdes, M., Elsby, R., Kakuta, S., Caceres, G., Saijo, S., Iwakura, Y., and Barber, G. N. (2007) *J. Immunol.* **178,** 6444–6455
5. Yoneyama, M., Kikuchi, M., Matsumoto, K., Imaizumi, T., Miyagishi, M., Taira, K., Foy, E., Loo, Y. M., Gale, M., Jr., Akira, S., Yonehara, S., Kato, A., and Fujita, T. (2005) *J. Immunol.* **175,** 2851–2858
6. Yoneyama, M., Kikuchi, M., Natsukawa, T., Shinobu, N., Imaizumi, T., Miyagishi, M., Taira, K., Akira, S., and Fujita, T. (2004) *Nat. Immunol.* **5,** 730–737
7. Hornung, V., Ellegast, J., Kim, S., Brzozka, K., Jung, A., Kato, H., Poeck, H., Akira, S., Conzelmann, K. K., Schlee, M., Endres, S., and Hartmann, G. (2006) *Science* **314,** 994–997
8. Pichlmair, A., Schulz, O., Tan, C. P., Naslund, T. I., Liljestrom, P., Weber, F., and Reis e Sousa, C. (2006) *Science* **314,** 997–1001
9. Saito, T., Hirai, R., Loo, Y. M., Owen, D., Johnson, C. L., Sinha, S. C., Akira, S., Fujita, T., and Gale, M., Jr. (2007) *Proc. Natl. Acad. Sci. U. S. A.* **104,** 582–587
10. Kawai, T., Takahashi, K., Sato, S., Coban, C., Kumar, H., Kato, H., Ishii, K. J., Takeuchi, O., and Akira, S. (2005) *Nat. Immunol.* **6,** 981–988
11. Meylan, E., Curran, J., Hofmann, K., Moradpour, D., Binder, M., Bartenschlager, R., and Tschopp, J. (2005) *Nature* **437,** 1167–1172
12. Seth, R. B., Sun, L., Ea, C. K., and Chen, Z. J. (2005) *Cell* **122,** 669–682
13. Xu, L. G., Wang, Y. Y., Han, K. J., Li, L. Y., Zhai, Z., and Shu, H. B. (2005) *Mol. Cell* **19,** 727–740
14. Rothenfusser, S., Goutagny, N., DiPerna, G., Gong, M., Monks, B. G., Schoenemeyer, A., Yamamoto, M., Akira, S., and Fitzgerald, K. A. (2005) *J. Immunol.* **175,** 5260–5268
15. Loo, Y. M., Fornek, J., Crochet, N., Bajwa, G., Perwitasari, O., Martinez-Sobrido, L., Akira, S., Gill, M. A., Garcia-Sastre, A., Katze, M. G., and Gale, M., Jr. (2008) *J. Virol.* **82,** 335–345
16. Komuro, A., and Horvath, C. M. (2006) *J. Virol.* **80,** 12332–12342
17. McWhirter, S. M., Tenoever, B. R., and Maniatis, T. (2005) *Cell* **122,** 645–647
18. Saha, S. K., Pietras, E. M., He, J. Q., Kang, J. R., Liu, S. Y., Oganesyan, G., Shahangian, A., Zarnegar, B., Shiba, T. L., Wang, Y., and Cheng, G. (2006) *EMBO J.* **25,** 3257–3263
19. Kayagaki, N., Phung, Q., Chan, S., Chaudhari, R., Quan, C., O'Rourke, K. M., Eby, M., Pietras, E., Cheng, G., Bazan, J. F., Zhang, Z., Arnott, D., and Dixit, V. M. (2007) *Science* **318,** 1628–1632
20. Lin, R., Yang, L., Nakhaei, P., Sun, Q., Sharif-Askari, E., Julkunen, I., and Hiscott, J. (2006) *J. Biol. Chem.* **281,** 2095–2103
21. Zhao, C., Denison, C., Huibregtse, J. M., Gygi, S., and Krug, R. M. (2005) *Proc. Natl. Acad. Sci. U. S. A.* **102,** 10200–10205
22. Arimoto, K., Konishi, H., and Shimotohno, K. (2008) *Mol. Immunol.* **45,** 1078–1084
23. Gack, M. U., Shin, Y. C., Joo, C. H., Urano, T., Liang, C., Sun, L., Takeuchi, O., Akira, S., Chen, Z., Inoue, S., and Jung, J. U. (2007) *Nature* **446,** 916–920
24. Urano, T., Saito, T., Tsukui, T., Fujita, M., Hosoi, T., Muramatsu, M., Ouchi, Y., and Inoue, S. (2002) *Nature* **417,** 871–875
25. Arimoto, K., Takahashi, H., Hishiki, T., Konishi, H., Fujita, T., and Shimotohno, K. (2007) *Proc. Natl. Acad. Sci. U. S. A.* **104,** 7500–7505
26. Sasai, M., Shingai, M., Funami, K., Yoneyama, M., Fujita, T., Matsumoto, M., and Seya, T. (2006) *J. Immunol.* **177,** 8676–8683
27. Douglas, J., Cilliers, D., Coleman, K., Tatton-Brown, K., Barker, K., Bernhard, B., Burn, J., Huson, S., Josifova, D., Lacombe, D., Malik, M., Mansour, S., Reid, E., Cormier-Daire, V., Cole, T., and Rahman, N. (2007) *Nat. Genet.* **39,** 963–965
28. Barral, P. M., Morrison, J. M., Drahos, J., Gupta, P., Sarkar, D., Fisher, P. B., and Racaniello, V. R. (2007) *J. Virol.* **81,** 3677–3684
29. Seol, J. H., Feldman, R. M., Zachariae, W., Shevchenko, A., Correll, C. C., Lyapina, S., Chi, Y., Galova, M., Claypool, J., Sandmeyer, S., Nasmyth, K., Deshaies, R. J., Shevchenko, A., and Deshaies, R. J. (1999) *Genes Dev.* **13,** 1614–1626
30. Pickart, C. M. (2004) *Cell* **116,** 181–190
31. Kim, M. J., Hwang, S. Y., Imaizumi, T., and Yoo, J. Y. (2008) *J. Virol.* **82,** 1474–1483
32. Alexopoulou, L., Holt, A. C., Medzhitov, R., and Flavell, R. A. (2001) *Nature* **413,** 732–738
33. Tanabe, M., Kurita-Taniguchi, M., Takeuchi, K., Takeda, M., Ayata, M., Ogura, H., Matsumoto, M., and Seya, T. (2003) *Biochem. Biophys. Res. Commun.* **311,** 39–48
34. Yoneyama, M., Suhara, W., Fukuhara, Y., Fukuda, M., Nishida, E., and Fujita, T. (1998) *EMBO J.* **17,** 1087–1095

Teleost TLR22 Recognizes RNA Duplex to Induce IFN and Protect Cells from Birnaviruses[1]

Aya Matsuo,[2]* Hiroyuki Oshiumi,[2]* Tadayuki Tsujita,[3]* Hiroshi Mitani,[†] Hisae Kasai,[‡] Mamoru Yoshimizu,[‡] Misako Matsumoto, and Tsukasa Seya[4]*

TLR22 occurs exclusively in aquatic animals and its role is unknown. Herein we show that the fugu (*Takifugu rubripes*) (fg)TLR3 and fgTLR22 link the IFN-inducing pathway via the fg Toll-IL-1R homology domain-containing adaptor protein 1(fgTICAM-1, or TRIF) adaptor in fish cells. fgTLR3 resides in endoplasmic reticulum and recognizes relatively short-sized dsRNA, whereas fgTLR22 recognizes long-sized dsRNA on the cell surface. On poly(I:C)-stimulated fish cells, both recruit fgTICAM-1, which in turn moves from the TLR to a cytoplasmic signalosome region. Thus, fgTICAM-1 acts as a shuttling platform for IFN signaling. When fish cells expressing fgTLR22 are exposed to dsRNA or aquatic dsRNA viruses, cells induce IFN responses to acquire resistance to virus infection. Thus, fish have a novel TICAM-1-coupling TLR that is distinct from the mammalian TLR3 in cellular localization, ligand selection, and tissue distribution. TLR22 may be a functional substitute of human cell-surface TLR3 and serve as a surveillant for infection with dsRNA virus to alert the immune system for antiviral protection in fish. *The Journal of Immunology*, 2008, 181: 3474–3485.

The type I IFN system is a host defense against microbial pathogens in animals (1, 2). In acute viral infections, IFN induces Mx and oligoadenylate synthetase to suppress viral replication (3). In late-phase infection it orchestrates cellular immunity including T and NK cells and protects hosts from persistent or repetitive viral infections (2, 4).

Earlier reports suggested that in mammalian fibroblasts, dsRNA (or its analog poly(I:C)) acts as an inducer for type I IFN, but the receptors for triggering IFN induction had not been identified until recently. Currently, in mammals, TLR3 on the endosomal membrane and retinoic acid-inducible gene I (RIG-I)[5] and melanoma differentiation-associated gene 5 (MDA5) in the cytoplasm are identified as sensors for dsRNA (1, 5). When viral genome RNA replicates in the cytoplasm, RIG-I and MDA5 sense it and assemble the adaptor mitochondrial antiviral signaling protein (MAVS; also called Cardif, IPS-1, orVISA) on the mitochondrial membrane (5). RIG-I preferentially recognizes 5′-phosphates of RNA (6, 7), whereas MDA5 recognizes the signature of dsRNA (8). They are distributed ubiquitously in cells/tissues and trigger IFN regulatory factor 3 (IRF-3) activation followed by type I IFN induction through the MAVS signal cascade (1, 2, 5). This intrinsic pathway appears to link main protective responses against RNA virus infection in mammals.

On the other hand, human TLR3 signals the presence of extrinsic dsRNA, recruits the adaptor Toll-IL-1R homology domain-containing adaptor protein 1 (TICAM-1), and induces IRF-3 activation followed by IFN-β promoter activation (1, 2, 9). Human TLR3 resides limitedly in myeloid dendritic cells, fibroblasts, and epithelial cells (10). TICAM-1 recruits TNF receptor-associated factor (TRAF) and TNF receptor-associated NF-κB kinase (TANK) family proteins for IFN-inducing signaling (11, 12; M. Sasai, H. Oshiumi, and T. Seya, unpublished data). NAK-associated protein 1 (NAP1), like other TANK family subunits (13), assembles two kinases, IKKε and TBK1, which activate the transcription factor IRF-3 (14). We call this extrinsic pathway the TICAM-1 pathway.

The TICAM-1 pathway and the cytoplasmic MAVS pathway converge on NAP1 to activate IRF-3 in human cells (15). Gene-disrupted mouse analyses show that TICAM-1 is involved in induction of the anti-mCMV immune response for host protection (16). The TICAM-1 pathway also appears to be involved in other DNA virus infections (16, 17). No clear involvement of TLR3 and TICAM-1 in defense against RNA virus infection has been offered using gene-disrupted mice, although many studies have anticipated that the TICAM-1 pathway has antiviral function against RNA viruses.

In fish studies, teleost IFN was recently discovered in the zebrafish (*Danio rerio*) (18), and since has been found in many fish species (19). Although the predicted protein sequence of the fish IFN has low

*Department of Microbiology and Immunology, Hokkaido University Graduate School of Medicine, Sapporo, Japan; †Department of Integrated Biosciences, University of Tokyo, Chiba, Japan; and ‡Faculty of Fisheries Sciences, Hokkaido University, Hakodate, Japan

Received for publication November 14, 2007. Accepted for publication June 20, 2008.

The costs of publication of this article were defrayed in part by the payment of page charges. This article must therefore be hereby marked *advertisement* in accordance with 18 U.S.C. Section 1734 solely to indicate this fact.

[1] This work was supported in part by CREST-JST (Japan Science and Technology Corporation), by Grants-in-Aid from the Ministry of Education, Science, and Culture (Specified Project for Advanced Research) and the Ministry of Health, Labor, and Welfare of Japan, and by the Takeda Science Foundation, Uehara Memorial Foundation, Northtec Foundation, Akiyama Foundation, and Mitsubishi Foundation. Financial support by the Sapporo Biocluster "Bio-S", the Knowledge Cluster Initiative of the MEXT, and the Program of Founding Research Centers for Emerging and Reemerging Infectious Diseases, MEXT, are gratefully acknowledged.

[2] A.Y. and H.O. contributed equally to this paper.

[3] Current address: Exploratory Research for Advanced Technology/Japan Science and Technology Center, Laboratory of Molecular and Developmental Biology, University of Tsukuba, Tennoudai 1-1-1, Tsukuba 305-8577, Japan.

[4] Address correspondence and reprint requests to Dr. Tsukasa Seya, Department of Microbiology and Immunology, Graduate School of Medicine, Hokkaido University, Kita-ku, Sapporo 060-8638, Japan. E-mail address: seya-tu@pop.med.hokudai.ac.jp

[5] Abbreviations used in this paper: RIG-I, retinoic acid-inducible gene I; BLAST, basic local alignment search tool; CPE, cytopathic effect; ER, endoplasmic reticulum; fg, *Takifugu rubripes*; HA, hemagglutinin; IPNV, infectious pancreatic necrosis virus; IRF-3, IFN regulatory factor 3; ISRE, IFN-stimulated regulatory element; LRR, leucine-rich repeat; MAVS, mitochondrial antiviral signaling protein; MDA5, melanoma differentiation-associated gene 5; moi, multiplicity of infection; NAP1, NAK-associated protein 1; PGN, peptidoglycan; rt, rainbow trout; polyC, polycytidylic acid; polyU, polyuridylic acid; $TCID_{50}$, 50% tissue culture-infective dose; TICAM-1, Toll-IL-1R homology domain-containing adaptor protein 1; TIR, Toll-IL-1 receptor; YFP, yellow fluorescent protein; zf, zebrafish.

(<20%) similarity to mammalian and avian type I IFNs, IFN-α and IFN-β, it up-regulates Mx and IFN-stimulated regulatory element (ISRE) promoter activation (18). Hence, fish possess IFN-inducing machinery. Since fish are exposed to viruses and RNA in water, they must have IFN-inducing receptors. However, no receptors for IFN induction have been identified yet in fish.

The existence of the TLR family in teleosts has been predicted from the genome database (20–23). According to the database of *Takifugu rubripes* (puffer fish), this teleost species possesses an ortholog of human TLR3 and other orthologs of human TLR members (20). Additionally, this teleost has a gene encoding a fish-specific TLR (hereafter called TLR22), whose functions are unknown. Fish may have a part of the gene of MDA5-like product, but its functional features are also unidentified. What happens in the IFN response during viral infection accordingly remains to be addressed in fish.

We found TLR22 in many aquatic vertebrate species (19, 20, 24), but not in birds and land animals (24). In this study, we demonstrate that TLR22 is a dsRNA-recognizing pattern receptor that recruits TICAM-1 to induce IFN and exerts a protective role in fish cells against dsRNA virus infection.

Materials and Methods

Accession numbers

Accession numbers for all genes used in this study are listed below: *T. rubripes* (fg)TLR22 (AB197916), rainbow trout (rt)TLR22-1 (AJ628348), rtTLR22-2 (AJ878915), rtTLR3 (DQ459470), rtIFN (AJ582754), and infectious pancreatic necrosis virus (IPNV) (NC001915). Rainbow trout has two orthologs of fgTLR22, rtTLR22-1 and rtTLR22-2, which were 93.0% homologous to each other (data not shown). Appropriate primers for detection of mRNAs of these genes are listed in Table I.

Cells and reagents

Human HEK293 or HeLa cells were cultured as described previously (10). A fibroblast-like cell line (OLHd-rRe3) of Japanese medaka fish, *Oryzias latipes*, was cultured in L-15 medium containing 20% heat-inactivated FCS and 10 mM HEPES at 33°C. RTG-2 cells derived from rainbow trout were cultured in a medium containing 10% heat-inactivated FCS and antibiotics (100 U/ml penicillin and 100 μg/ml streptomycin) at 20°C. LPS was purchased from BD Biosciences. Peptidoglycan (PGN) was purified from *Staphylococcus aureus* (Fluka). All nucleotide primers and oligodeoxynucleotides (ODN) containing CpG motifs (CpG-ODN) were purchased from Sigma-Genosys. Poly(I:C), polycytidylic acid (polyC), polyuridylic acid (polyU), and poly(dI:dC) were purchased from Amersham Biosciences. Variable-sized dsRNAs were transcribed from a cDNA template of measles virus with MEGAscript (Ambion) in vitro.

Molecular cloning of T. rubripes *DNAs*

First-strand cDNAs were reverse-transcribed from random-primed RNA templates extracted from *T. rubripes* kidney or eye tissues using M-MLV(−) reverse transcriptase (Promega). FgTLR3, fgTLR22, and fgTICAM-1 full-length cDNA fragments were amplified by PCR using primers shown in Table I. The PCR products were cloned using pCR-Blunt vector (Invitrogen). Several independent clones were subjected to DNA sequencing using ABI 3100 sequencer (PE Applied Biosystems) for assessing sequence accuracy. IFN of *T. rubripes* was searched by homology to zebrafish IFN using the basic local alignment search tool (BLAST) server. The 5′ promoter region identified from *T. rubripes* genomic DNA as −1 to −777 was subcloned into pEFBOS vector. FgMyD88 Toll-IL-1 receptor (TIR) domain was found in the *T. rubripes* database by BLAST search with reference to the human MyD88 protein sequence, and amplified by PCR using the primers shown in Table I.

cDNA expression vector

The cDNAs encoding fgTLR3 and fgTLR22 were placed between the *Xho*I and *Not*I sites of the pFEBOS expression vector. Flag-, hemagglutinin (HA)-, and Myc-tags were attached to the C- or N-terminus of the proteins as described previously (15, 25). Constitutively active CD4/TLR22 was constructed by fusing cDNAs encoding the extracellular domain of huCD4 (from 1 to 391 aa region) to the transmembrane and cytoplasmic domains of fgTLR22 (from 565 to 935 aa region). The obtained chimera CD4/TLR22 construct was placed between the *Xho*I and *Not*I sites of pEFBOS. Flag-tag was inserted just before the stop codon of fgTLR22 and placed between the *Xho*I and *Not*I sites of pEFBOS. To make the fgTLR22-myc expression vector, myc-tag was added to the C-terminal end of the signal peptide sequence of fgTLR22 and subcloned into *Xho*I and *Not*I sites of the pEFBOS expression vector. FgTLR3-yellow fluorscent protein (YFP) expression vector was constructed by inserting the full-length fgTLR3 into the pEYFP-N1 vector at the *Xho*I and *Kpn*I sites. The constructs of the dominant-negative human TICAM-1 (TICAM TIR (P434H)) and MyD88 (TIR) were described previously (25). Dominant-negative forms of fgTICAM-1 and fgMyD88 were constructed as human dominant-negative counterparts. Precisely, cDNA encoding the 341–479 aa region of fgTICAM was inserted into the pEFBOS *Xho*I-*Not*I sites and substituted proline at 382 with histidine. The fgMyD88 TIR domain-encoding region (152–288 aa region) was subcloned into the *Xho*I-*Not*I sites of pEF-BOS.

Table I. *Primer list*

Primer Name[a]	Sequence
fgTLR22-F	CTCAGAGCTTTGTGGTGTCT
fgTLR22-R	TTGCTTCTCTGATTAAGCCC
fgTLR3-F	CCAAGTGAAAACCACACGCA
fgTLR3-R	CTGGGACAACGGGACCTTT
fgTICAM-F	CATCTCTGCTGAATGGGG
fgTICAM-R	GTGGTGTAATGGACTGTAG
fgMyD88-F	CTCGGTAGGTCCAGTTTTC
fgMyD88-R	TCCTGCACCATATTCTGC
fgIFN promoter-F	TTGAATGGAAACAAGTCAGT
fgIFN promoter-R	CTTTCACTCAAGGAGGTCGC
rtIFN-F	CTGACCGGATGCAGAAGGA
rtIFN-R	TGGAGAGAGAAGCCAAGATGGA
rtTLR22-F	CTTTGATGAGCAGAAGGACG
rtTLR22-R	CTAAAGCCAGCCGTAGTTGC
rtβ-actin-F	CCTGTGTATCACCTGCCATGA
rtβ-actin-R	ACGCCTGTGCACTGTAGTTCA

[a] F indicates forward; R, reverse.

Reporter gene assay

HEK293 cells (1×10^6 cells/well) were transiently transfected in 24-well plates using Lipofectamine 2000 reagent (Invitrogen) with pEFBOS human TLR2, human TLR3, human TLR4, human TLR9, fgTLR3, fgTLR22 (200 ng), dominant-negative human TICAM-1 (P434H), human MyD88 (TIR) (50, 200 ng) or empty vector, together with a luciferase-linked IFN-β promoter gene (Stratagene, 100 ng). RTG-2 cells (1×10^6 cell/well) were transiently transfected in 24-well plates using FuGene HD (Roche) with fgTLR22, fgTLR3 (200 ng), dominant-negative fgTICAM-1 (50 or 200 ng), or empty vector together with a luciferase-linked fgIFN promoter gene. In some experiments, stable clones with this gene (named RTG (Luc-fgIFN) cells) were used instead of human IFN reporter. phRL-TK vector (1 ng) (Promega) was used as an internal control. Twenty-four hours after transfection, cells were stimulated with LPS (100 ng/ml), PGN (10 μg/ml), CpG (2 mM), or poly(I:C) (10 or 50 μg/ml), polyC (10 μg/ml), polyU (10 μg/ml), poly(dI:dC) (10 μg/ml), and in vitro-transcribed dsRNA (typically 10 μg/ml) for 6 h. The cells were lysed with lysis buffer (Promega) and luciferase activity was measured using a dual-luciferase reporter assay kit (Promega) with luminometer (Berthold Technologies). Specific activity was calculated from light intensity measurements with a *Renilla* luciferase internal control. Values were expressed as mean relative stimulation with SD from triplicate values from a minimum of three separate experiments.

Confocal microscopy

HeLa, OLHd-rRe3, and RTG-2 cells were plated onto coverglass in a 24-well plate. In the following day, cells were transfected with indicated plasmids using FuGene HD. The amount of DNA was kept constant by adding empty vector. After 24 h, cells were stimulated with poly(I:C) and fixed with 3% of formaldehyde in PBS as indicated periods, and then washed four times with PBS. Cells were permeabilized with PBS containing 0.2% Triton X-100 for 15 min. Permeabilized cells were blocked with PBS containing 1% BSA, and were labeled with anti-Flag mAb (Sigma-Aldrich) or anti-HA pAb (Sigma-Aldrich) in 1% BSA/PBS for 1 h at room temperature. The cells were then washed with 1% BSA/PBS and treated for 30 min at room temperature with Alexa-conjugated Abs (Molecular Probes). For

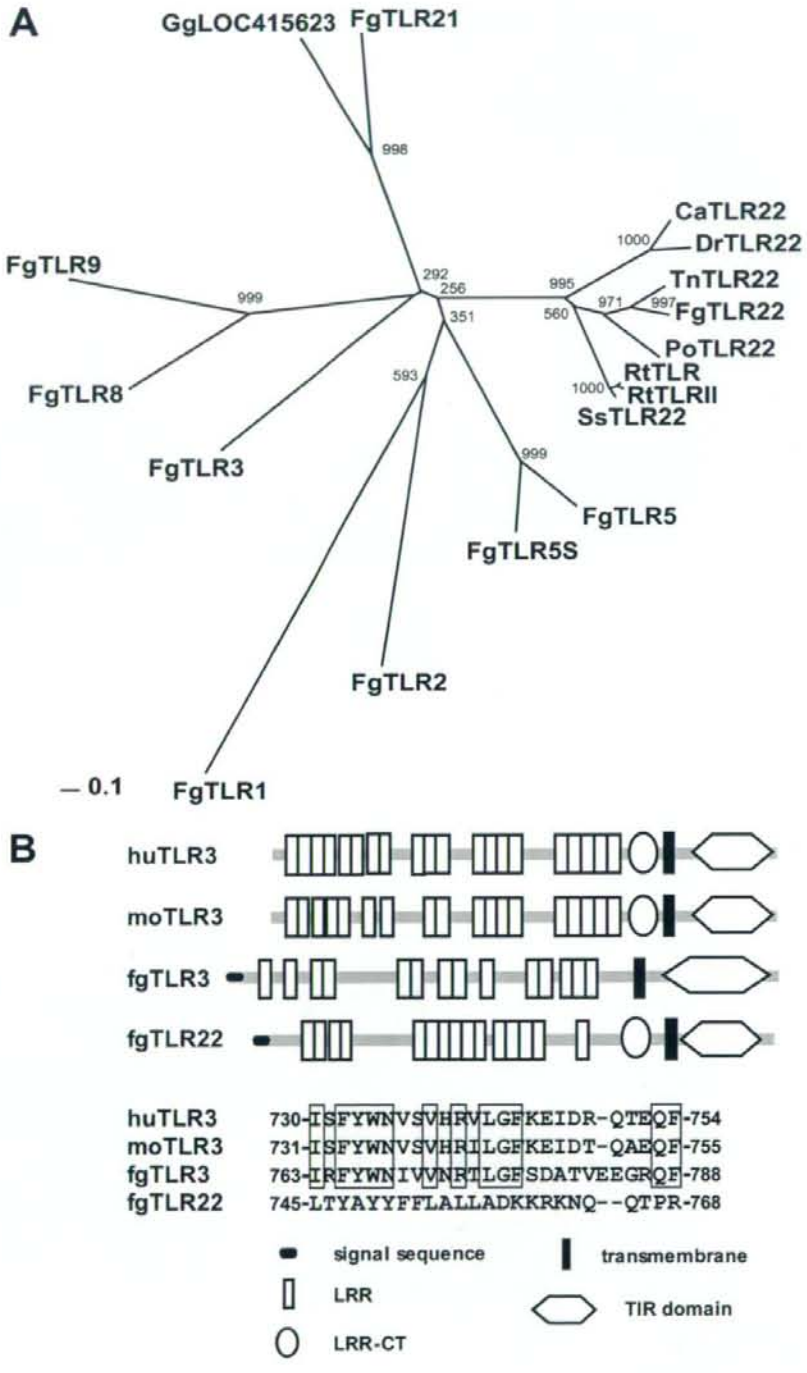

FIGURE 1. Structures and phylogenic analysis of TLR3 and TLR22. *A*, Gene tree for fgTLR22. Teleost and chicken TLR protein sequences were aligned with ClustalW on DDBJ server, and the phylogenic tree was made by a neighbor-joining method program. Number on each node represents bootstrap probability that is 1000× reiteration. Fg, Ca, Dr, Tn, Po, Rt, and Ss stand for *Takifugu rubripes*, *Carassius auratus*, *Danio rerio*, *Tetradon nigroviridis*, *Paralichthys olivaceus*, rainbow trout, or *Salmo salar*. GgLOC415623 is a chicken protein that is most similar to fgTLR22. The protein was classified into TLR21 by the phylogenic tree. *B*, Motif structures of human, mouse, and fugu TLR3 and fugu TLR22. Possible domain structures of the fish TLRs were obtained with SMART search according to the primary sequences. Vertical open bars represent LRRs and filled bars represent transmembrane domains. LRR-CT (the leucine-rich repeat at the C terminus) is shown by circles. The signal sequences are shown to the left and TIRs are to the right. Amino acid sequence alignment of the linker regions of huTLR3, moTLR3, fgTLR3, and fgTLR22 are shown at the bottom.

organelle marker staining, cells were treated with calnexin (StressGen Biotechnologies) and then FITC-labeled goat anti-mouse IgG secondary Ab. In some cases cells were prestained with anti-TLR Abs. Thereafter, microcoverglasses were mounted onto a slide glass using PBS containing 2.3% 1,4-diazabicyclo(2.2.2)octane (DABCO) and 50% of glycerol. In some experiments, we used YFP-labeled fgTLR3 instead of tagged fgTLR3, since the background by the secondary Ab (against tag) was increased for unknown reasons in the case of fgTLR3. The stained cells were visualized at ×60 magnification under a FluoView (Olympus).

Isolation of IPNV RNA

IPNV was propagated with RTG-2 cells. RTG-2 cells cultured in a 75-cm^2 T flask were infected with IPNV. After 4–7 days incubation, viruses were

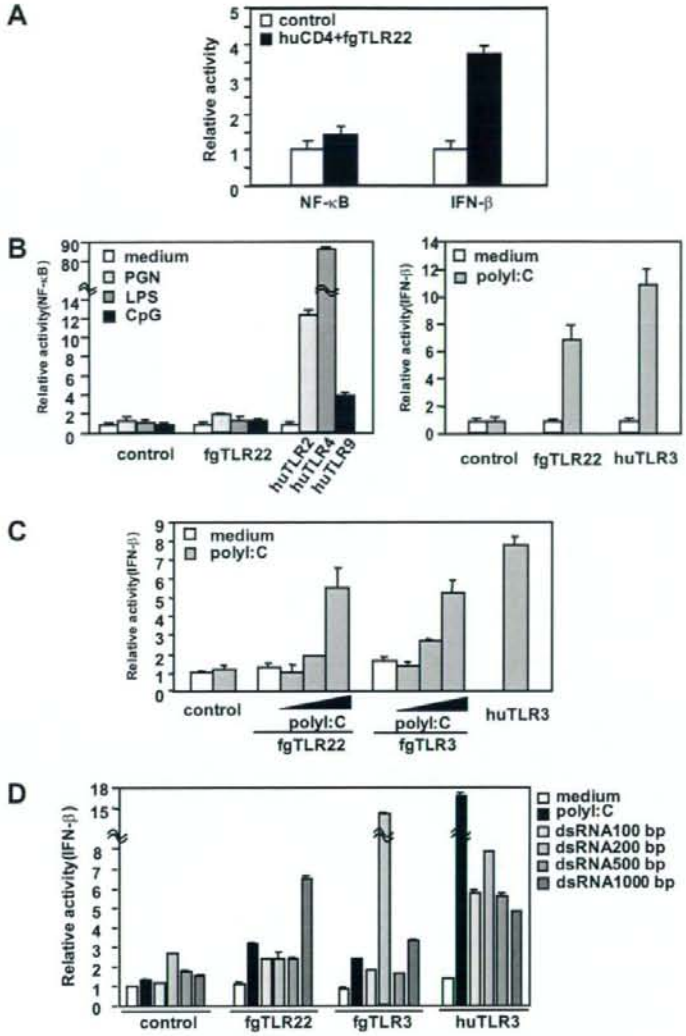

FIGURE 2. Human cells expressing fgTLR22 induce activation of the human IFN-β promoter in response to poly(I:C). *A*, HEK293 cells were transfected with expression vector for CD4 + TLR22, where the cytosolic domain of fgTLR22 (the TIR domain) was fused to the extracellular portion of CD4. The amount of DNA transfected was equalized with empty expression vector, which was also used as the control. Reporter activity was determined as described in the text. *B*, HEK293 cells were transfected with fgTLR22 (full-length)-expressing vector or pEFBOS (vector only). Twenty-four hours after transfection, cells were stimulated with PGN (10 μg/ml), LPS (100 ng/ml), and CpG (2 μM) for 6 h and NF-κB promoter activation was determined (*left panel*). *Right panel*, poly(I:C) (50 μg/ml) was used instead of other stimulators, and relative IFN-β promoter activation by poly(I:C) was compared between fgTLR22 and human (hu)TLR3. *C*, HEK cells were transfected with the vector for expression of huTLR3, fgTLR22, or fgTLR3. pEFBOS and pEFBOS (huTLR3) were used as controls. Twenty-four hours after transfection, cells were stimulated with poly(I:C) (5, 10, 50 μg/ml) for 6 h. IFN-β promoter activation was measured by luciferase activity in the cell lysates. *D*, Cells were transfected with full-length fgTLR22- or fgTLR3-expressing vector. pEFBOS was a control for vector only. Twenty-four hours later, cells were stimulated with 10 μg/ml of poly(I:C) or variable-sized (100-, 200-, 500-, and 1000-bp) dsRNA for 6 h. IFN-β promoter activation was measured by luciferase assay as in *C*.

harvested from infected cell lysates by freeze-thaw cycles. Cell debris was removed by centrifugation at 10 krpm for 10 min, and then virus particles were concentrated by ultracentrifuge at 23 krpm for 1 h. Viral RNA was extracted from 15 ml of these lysates with 500 μl of TRIzol (Invitrogen) according to the manufacturer's instructions.

Quantitative PCR

Total RNA of RTG-2 cells were extracted using TRIzol reagents, and cDNA was made by using MV-reverse transcriptase with random primers. iQ SYBER Green Supermix was used for PCR reactions and analyzed with iCycler iQ real-time PCR analyzing system (Bio-Rad). Primers for quantitative PCR are shown in Table I. Relative rtIFN mRNA levels were calculated by dividing the relative amounts of mRNA of rtIFN by those of the rainbow trout β-actin mRNA.

Immunoprecipitation

HEK293FT cells were transiently transfected with expression vectors in a 6-well plate using Lipofectamine 2000 reagent (Invitrogen) and incubated for 24 h. Cells were lysed with lysis buffer (25 mM Tris-HCl (pH 7.5), 150 mM NaCl, 1% of Nonidet P-40, 2 mM PMSF, 25 mM iodoacetaminde, 10 mM EDTA), and proteins were immunoprecipitated with anti-Flag mAb and then washed four times with lysis buffer. Obtained samples were analyzed by SDS-PAGE (7.5 or 10% gel) and Western blotting using anti-HA pAb (Sigma-Aldrich).

Titration of virus

RTG-2 cells (1×10^6 cells/well) were infected with IPNV (typical multiplicity of infection (moi) of 0.1). After 24 h, supernatants were serially 10-fold diluted and incubated with RTG-2 cells placed on a flat 96-well plate, and 100 μl medium with 8× dilution cycles was added to determine the 50% tissue culture-infective dose ($TCID_{50}$). Cells were incubated at 15°C for 7 days. On day 7 of incubation, the plates were examined for the presence of viral cytopathic effect (CPE) under the microscope.

Results

Identification of TLR22 in T. rubripes

We used the predicted protein sequence of fgTLR22 for a BLASTP search on the National Center for Biotechnology Information (NCBI) BLAST server for a nonredundant database, and found that teleosts and frogs (*Xenopus tropicalis*) have TLR22 orthologs by phylogenetic analyses (20, 24) (Fig. 1*A*). However, no expressed sequence tag or genome region encoding TLR22 was

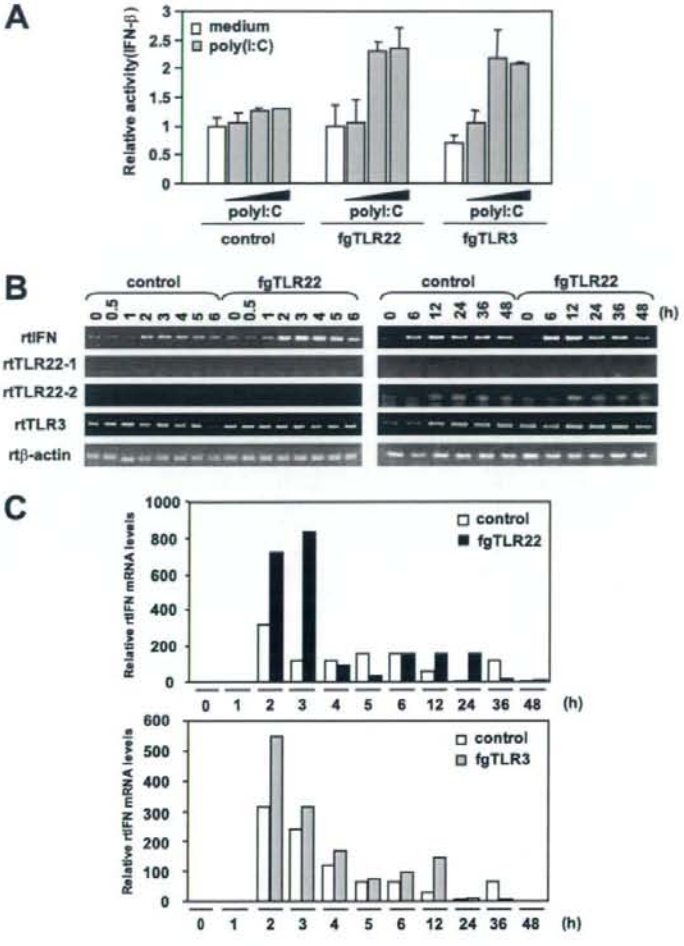

FIGURE 3. fgTLR22 recognizes poly(I:C) to induce fish IFN in fish cells. *A*, Rainbow trout RTG-2 cells were stably transfected with Luc-fgIFN vector (see *Materials and Methods*). The RTG (Luc-fgIFN) cells were then transiently transfected with fgTLR22 or fgTLR3 expression vector or control pEFBOS. Twenty-four hours later, cells were stimulated with poly(I:C) (5, 10, 50 μg/ml) for 6 h, and fgIFN promoter activation was determined by luciferase activity in the cell lysate. *B*, RTG-2 cells were transiently transfected with fgTLR22-expressing vector or control pEFBOS. Twenty-four hours later, cells were stimulated with poly(I:C) (25 μg/ml) for the indicated intervals. Since the rainbow trout possesses two mRNAs of TLR22, we referred them to rtTLR22–1 and rtTLR22–2. The mRNA levels of rtIFN, rtTLR22–1, rtTLR22–2, rtTLR3, and rtTICAM-1 were monitored by RT-PCR. The rtTICAM-1 message was constitutively expressed irrespective of poly(I:C) stimulation (data not shown). rtβ-actin was used for the control. PCR products were analyzed by gel electrophoresis (1.5% TAE agarose) and visualized with ethidium bromide (1 μg/ml). Three individual experiments were performed, and a representative one is shown. *C*, RTG-2 cells were transfected with pEFBOS (fgTLR22), pEFBOS (fgTLR3), or empty pEFBOS. Twenty-four hours later, cells were stimulated with poly(I:C) (25 μg/ml) for the indicated periods. The mRNA levels of rtIFN were measured by quantitative PCR. Relative fold induction against rtβ-actin level is shown. The experiments were performed three times and representative results are shown.

found in mammals and birds. Thus, these homology search analyses indicate that the TLR22 gene is conserved across aquatic vertebrates. To further confirm the absence of the TLR22 gene in the chicken genome, we conducted a TBLASTN search with fgTLR22 against the *Gallus gallus* whole genome. The best hits sequence in the chicken genome was the region encoding LOC415623, but the protein was an ortholog of TLR21 (data not shown). In the mouse genome, the most similar sequence to fgTLR22 was mouse TLR13. These analyses confirmed that TLR22 is conserved in vertebrates living in water or wet conditions, but not in animals living on land.

We cloned the fgTLR22 cDNA from the kidney and eye of *T. rubripes* to test its function. The cDNA sequence of the isolated fgTLR22 was identical to the sequence we previously predicted, and its open reading frame was encoded by three exons (20). The fgTLR22 protein had 15 leucine-rich repeats (LRRs) and one C-terminal LRR domain at the extracellular region and a TIR domain in the cytoplasmic region, suggesting that fgTLR22 possesses a typical structure of TLR but differs in the primary structure from TLR3 (Fig. 1*B*).

IFN promoter activation by fgTLR22 in a human cell line

Vertebrate IFN promoter and NF-κB activation has been determined successfully using human cells that have the human TLR signal system (26, 27). Thus, we first tested the functional ability of the TIR domain of fgTLR22 in human cell line HEK293. To estimate the output of fgTLR22 signaling, we made a chimera protein in which the Ig-like domain of CD4 was ligated with the transmembrane and intracellular region of fgTLR22. The human TLR4-CD4 chimera construct is known to activate the downstream signal of TLR4 by dimerization of the extracellular CD4 region (28). We examined whether the CD4-fgTLR22 chimera protein activates the human IFN-β promoter or NF-κB. The chimera protein was coexpressed in human HEK293 cells with an IFN-β promoter or NF-κB reporter plasmid. We observed minimal activation of NF-κB and about a 4-fold significant activation of the IFN-β promoter by expression of the chimera protein (Fig. 2*A*), suggesting that the TIR domain of fgTLR22 retains the capacity to activate the human IFN-β promoter and, to a lesser extent, the transcription factor NF-κB in human cells.

Ligand properties of fgTLR22 in comparison with those of fgTLR3

The functional ability of fgTLR22 in HEK293 cells encouraged us to look for the ligand of fgTLR22. We subcloned the fgTLR22 full-length cDNA into the expression vector pEFBOS and transfected it into human HEK293 cells with reporter plasmids. FgTLR22 or mock-transfected cells were stimulated with PGN,

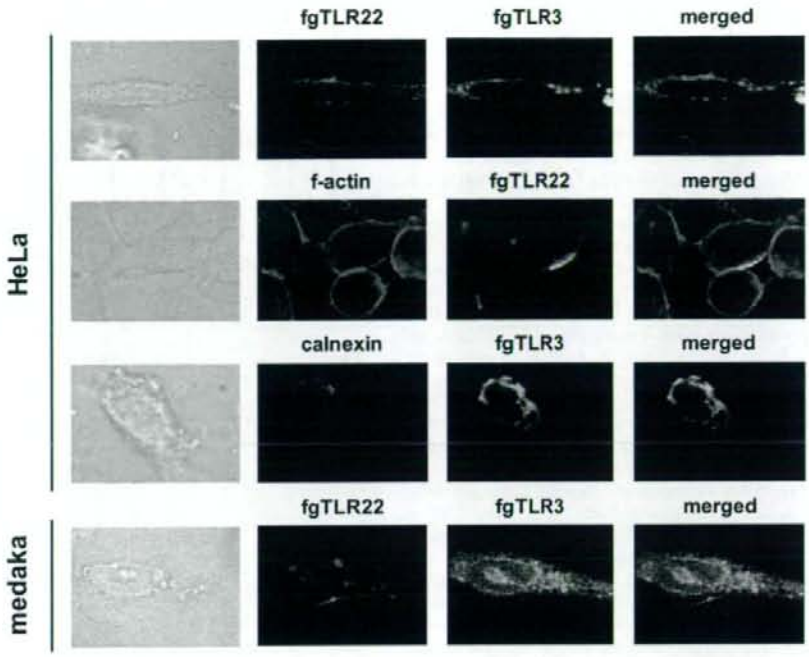

FIGURE 4. Localization of fgTLR22 and fgTLR3 in mammalian and fish cells. Confocal analysis using HeLa or medaka cells (OLHd-rRe3). fgTLR22 with C-terminal Flag, fgTLR3 with C-terminal YFP (green), and/or other markers were expressed in the indicated cells. fgTLR22 was labeled with mouse anti-Flag mAb and stained with Alexa 568-conjugated (red) or Alexa 488-conjugated (green, only in the second column) goat anti-mouse IgG. Cells were then treated with mAbs against Calnexin (ER marker) or f-actin (cytoskeleton marker) and Alexa 568-conjugated goat anti-mouse IgG. Phase-contrast features of cells are shown to the left. Cells were analyzed on FluoView.

LPS, CpG, or poly(I:C) for 6 h, and cell lysates were then prepared to measure reporter activation. PGN, LPS, and CpG activated neither NF-κB nor the IFN-β promoter via fgTLR22, although they activated the reporter via stimulation of the relevant human TLRs. In contrast, only poly(I:C) significantly activated the IFN-β promoter in fgTLR22-expressing cells (Fig. 2*B*). Thus, poly(I:C) is a ligand for fgTLR22. Because *T. rubripes* possesses an ortholog of TLR3 (20), we cloned fgTLR3 and measured the IFN-β promoter activation induced by poly(I:C) in fgTLR3-expressing cells. fgTLR3 also conferred the responsiveness to poly(I:C) on HEK293 cells in a way similar to fgTLR22 (Fig. 2*C*). Hence, the *T. rubripes* possesses two types of TLRs that recognize poly(I:C).

We next compared the response of fgTLR3 and fgTLR22 to polyU, polyC, poly(dI:dC), poly(I:C), and dsRNA using HEK transfectants. Ultimately, poly(I:C) and in vitro-transcribed dsRNA, but not polyU, polyC, or poly(dI:dC), activated the reporter in fgTLR22- or fgTLR3-expressing cells (data not shown), suggesting that both fgTLR22 and TLR3 signal the presence of dsRNA in human cells.

Next, we used various sizes of in vitro-transcribed dsRNA (29). Human TLR3 activated reporter genes in response to variable-sized dsRNA to similar extents irrespective of the length of dsRNA. In contrast, fgTLR22 and fgTLR3 showed different properties on responsiveness to variable-sized dsRNAs. In fgTLR22-expressing cells, 1000-bp dsRNA most strongly activated the reporter gene, but in fgTLR3-expressing cells, 200-bp dsRNA induced preferential activation of the reporter (Fig. 2*D*). Therefore, fgTLR3, fgTLR22, and human TLR3 exhibit differences in preference to the size of dsRNA, although the three TLRs essentially confer response to poly(I:C) or dsRNA on HEK293 cells. These observations using the human cell indicate a unique role of fgTLR22 in poly(I:C) or dsRNA recognition.

IFN induction by fgTLR22 in fish cells

We assessed the function of fgTLR22 in a teleost fibroblastic cell line, RTG-2. Teleosts also have an ortholog of human IFN, but previous phylogenetic analyses suggest that fish IFN forms a clade distinct from that of mammalian type I IFNs (18). The zebrafish (zf) IFN can be induced by overexpression of zfTICAM-1 (30), and it exerts antiviral effects through the induction of antiviral protein like Mx (31). We cloned the promoter region of the *T. rubripes* IFN gene that corresponds to the zfIFN and fused it to the luciferase open reading frame. fgTLR22 is widely expressed in various tissues and cell lines (20). Of the cell lines tested, the rainbow trout cell line, RTG-2, expressed only minute levels of the rtTLR22/rtTLR3 messages, which allowed us to employ RTG-2 for the fgTLR3/22 reporter analyses.

The RTG-2 cells were transfectable, but the transfection efficacy was ~10% by lipofection. fgTLR22 protein showed 80.8% similarity to rtTLR22 (rtTLR22-1 and rtTLR22-2), which was barely expressed in both unstimulated and poly(I:C)-stimulated cells (see Fig. 3*B*). The TIR sequences of fgTLR22 and rtTLR22 were 93.8% similar (data not shown), suggesting that they are functionally compatible. We transfected fgTLR22, fgTLR3, or mock expression vectors into RTG-2 cells together with the fgIFN promoter reporter plasmid (Fig. 3*A*). At 24 h after transfection, cells were stimulated with poly(I:C). Cell lysate was prepared 6 h after poly(I:C) stimulation, and luciferase activities were measured. Poly(I:C) barely activated the fgIFN reporter in control cells, but significantly activated it in fgTLR22- or fgTLR3-transfected cells (Fig. 3*A*), as observed in the human reporter assay system.

We next examined whether fgTLR22 transmits the signal to the endogenous IFN promoter (Fig. 3*B*). The NCBI DNA database has two cDNA sequences of the IFN gene in rainbow trout (AJ582754 and AM235738). We examined the poly(I:C)-inducible IFN (AJ582754) expression through fgTLR22 stimulation with poly(I:C) by RT-PCR analysis. RTG-2 cells transfected with fgTLR22 or empty vectors were incubated with medium containing poly(I:C), and expression of rtIFN was examined by RT-PCR and quantitative PCR. The IFN mRNA expression was more strongly increased 2 h after poly(I:C) stimulation in fgTLR22-expressing cells

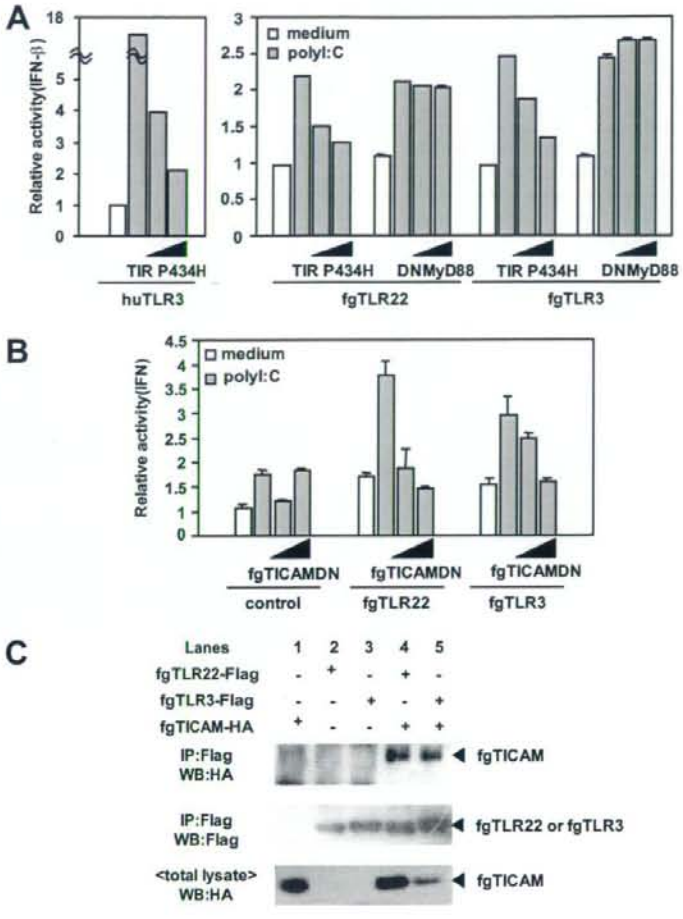

FIGURE 5. fg/huTICAM-1 is the adaptor for fgTLR22- and fgTLR3-mediated IFN promoter activation. *A*, Human (hu)TICAM-1 transmits signal for IFN-β promoter activation by fgTLR3 and fgTLR22 in HEK293 cells. HEK293 cells were transfected with fgTLR22 or fgTLR3 plasmid together with the plasmid encoding dominant-negative forms of huTICAM-1 or huMyD88. huTLR3 and TIR P434H were used as controls (*right panel*). Twenty-four hours later, cells were stimulated with poly(I:C) (10 μg/ml) for 6 h, and IFN-β promoter activation was determined by luciferase activity in the cell lysate. *B*, fgTICAM-1 acts as the adaptor for fgTLR3 and fgTLR22 to activate the fgIFN promoter in response to poly(I:C) in RTG-2 cells. RTG-2 cells were transfected with pEFBOS (fgTLR22), pEFBOS (fgTLR3), or pEFBOS together with dominant-negative forms of fgTICAM-1. After 24 h, cells were stimulated with poly(I:C) (10 μg/ml) for 6 h, and fgIFN promoter activity was determined by luciferase activity in cell lysate. *C*, fgTICAM-1 physically binds fgTLR3 and fgTLR22. HEK293 cells were transfected with plasmid with fgTLR22 or fgTLR3 together with plasmid of fgTICAM-1. Lysates from the cells transfected with the indicated vectors were immunoprecipitated (IP) with anti-Flag Ab and the samples were resolved on SDS-PAGE and analyzed by immunoblotting, which were probed with anti-HA Ab (*top panel*) or anti-Flag Ab (*middle panel*). fgTICAM-1 was detected in the blot of the total lysate by anti-HA Ab (*bottom panel*). Protein bands were developed by ECL kit. Arrows indicate HA-tagged fgTICAM-1 (*top and bottom panels*); Flag-tagged fgTLRs (*middle panel*).

than in control cells, and then gradually decreased in both types of cells (Fig. 3*B*).

Because human TLR3 expression is induced by poly(I:C) (32), we investigated whether teleost TLR22 or TLR3 transcriptions are activated by poly(I:C) stimulation. Endogenous rtTLR22 or rtTLR3 expression was scarcely observed without stimulation, and rtTLR22 expression was induced from 12 h after stimulation. rtTLR3 was also up-regulated but more mildly than fgTLR22 in response to poly(I:C) stimulation (Fig. 3*C*). These data are consistent with the notion that TLR22 is involved in the dsRNA recognition pathway.

Localization of fgTLR3 and fgTLR22

Why are there two TLRs that respond to poly(I:C) or dsRNA in teleosts? The answer may lie in the differences between the two TLRs. fgTLR3 and fgTLR22 preferentially recognize different sizes of dsRNA, as suggested by the reporter analyses. An additional difference is that fgTL22 localizes to the surface of the cell membrane while fgTLR3 localizes inside the cell. TLRs are type I transmembrane proteins, and their subcellular localizations are determined based on their primary structures and coupling proteins (33, 34). Human TLR1, 2, 4, 5, and 6 are expressed on the cell surface, but TLR3, 7, and 9 are mainly localized at intracellular compartments, endoplasmic reticulum (ER), and early endosomes (10, 35). In the case of human TLR3, its linker region between the transmembrane and TIR domain is a critical determinant for its localization (33). Human TLR3 and fgTLR3 share similar linker regions, but fgTLR22 does not have a similar linker sequence (Fig. 1*B*). Thus, we expected that fgTLR22 and fgTLR3 are distinctly localized.

To test this premise, we transfected HEK293 cells with myc-tagged fgTLR22 or Flag-tagged fgTLR3 and examined their expression using FACS analysis. fgTLR22 protein was observed partially on the cell surface (data not shown). On the cell surface, however, no fgTLR3 expression was observed, consistent with the case of dendritic cell human TLR3, which resides in the cytoplasmic compartments. Next, we overexpressed fgTLR22 or fgTLR3 in HeLa cells and visualized their localizations using a confocal microscope. YFP-labeled fgTLR3 was used in this study to avoid artificial deposition of fluorescence-labeled secondary Abs onto the cells. YFP labeling and HA or Flag labeling gave a similar imaging profile to fgTLR3 (data not shown). fgTLR3 was localized in the cytoplasm (Fig. 4). FgTLR3 was largely merged with calnexin (an integral protein localized in ER), suggesting that fgTLR3 localizes in the ER. In contrast, fgTLR22 was largely situated in close proximity to the cell surface, with only a minor population sitting in the cytoplasm (Fig. 4). These results confirm the predominant localization of fgTLR22 on the cell surface.

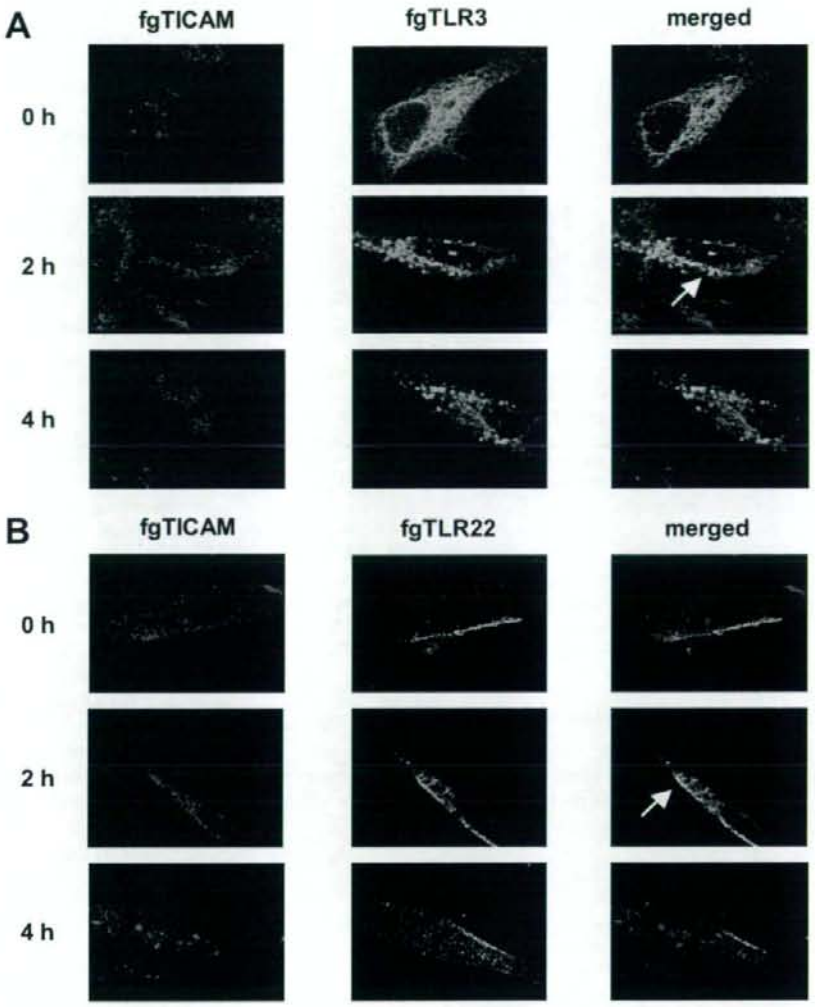

FIGURE 6. Dynamics of fgTICAM-1, fgTLR22, and fgTLR3 after poly(I:C) stimulation. RTG-2 cells onto coverslips were transfected with fgTLR22 (Flag-tagged) and fgTICAM-1 (HA-tagged) (*A*) or fgTLR3 (YFP) and fgTICAM-1 (HA-tagged) (*B*). Cells were allowed to stand for 24 h, stimulated with poly(I:C) (25 μg/ml) for the indicated intervals, and then stained with anti-Flag mAb and anti-HA pAb. Samples were analyzed by confocal microscopy. YFP and Flag labeling gave a similar localization profile to TLR3 (data not shown).

In the next experiment, we transfected OLHd-rRe3 fibroblastic cells derived from *O. latipes* (36) with fgTLR22 or fgTLR3 and tested their localizations. Although the transfection efficacy was very low in OLHd-rRe3 cells, we checked localization of TLRs by confocal analysis. As in the HeLa cells, cytoplasmic localization of fgTLR3 and cell surface-dominant localization of fgTLR22 were confirmed with OLHd-rRe3 cells (Fig. 4). Double staining of both fgTLR22 and fgTLR3 clearly supported their differential localizations. We also observed these localization differences in RTG-2 cells (data not shown). Taken together, fgTLR22 mainly localizes on the cell-surface membranes distinct from fgTLR3 in fish cells.

Adaptor selection of fgTLR22

Human TLR family proteins use four adaptor proteins, MyD88, Mal/Toll-IL-1R domain-containing adaptor protein (TIRAP), TICAM-1/TRIF, and TICAM-2/TRAM, to induce cytokine production (1, 2). Several teleost genomes encode three adaptor proteins, MyD88, TIRAP, and TICAM-1 (37). Teleost TICAM-2 has not been found and may have been lost in the teleost lineage during evolution (30). At first we used HEK293 cells to determine which human adaptor protein is compatible with fgTLR22 by reporter assay. FgTLR22 and a dominant-negative form of human MyD88 or TICAM-1 were transfected into HEK293 cells with the human IFN-β promoter reporter, and the cells were stimulated with poly(I:C). The dominant-negative form of human TICAM-1 (P434H) inhibited IFN-β promoter activation in fgTLR22-expressing cells, but the dominant-negative human MyD88 did not (Fig. 5*A*). Additionally, P434H inhibited fgTLR3-mediated IFN-β promoter activation in fgTLR3-expressing HEK293 cells (Fig. 5*A*). Thus, human TICAM-1 can act as an adaptor for fgTLRs.

Next, we made the dominant-negative form of fgTICAM-1, which has a mutation similar to that of the human dominant-negative form. We transfected fgTLR22, fgTLR3, and type I IFN reporter into RTG-2 cells with or without the dominant-negative form of fgTICAM-1 and then examined reporter activation. As in human cells, dominant-negative fgTICAM-1 inhibited the reporter activation in fgTLR22- and fgTLR3-transfected cells (Fig. 5*B*). Hence, fgTLR22 and fgTLR3 used fgTICAM-1 as the adaptor.

To further confirm the utilization of fgTICAM-1 as the adaptor by fgTLR22, we performed immunoprecipitation analyses. Full-length Flag-tagged fgTLR22 or fgTLR3 was transfected into HEK293 cells together with HA-tagged full-length fgTICAM-1.

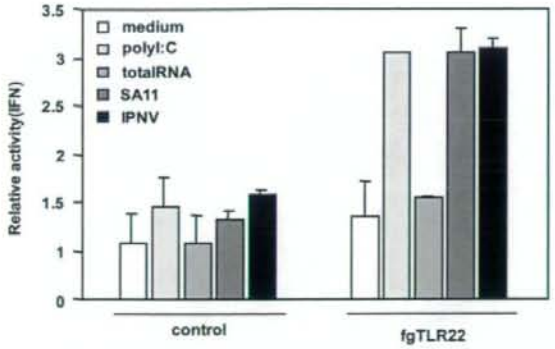

FIGURE 7. Viral dsRNA-mediated fgIFN induction interferes with fgTLR22. RTG-2 cells were transfected with the fgTLR22 plasmid (pEFBOS (fgTLR22)) or pEFBOS (vector only) and the fgIFN reporter plasmid. Twenty-four hours later, cells were treated for 6 h with medium only, poly(I:C), RTG-2 cell total RNA, or dsRNA of IPNV or rotavirus (SA11) origin. fgIFN activation was monitored by luciferase activity in the cell lysate.

We prepared cell lysates 24 h after transfection, and fgTLR22 and fgTLR3 were immunoprecipitated with anti-Flag Ab. Precipitates were analyzed by SDS-PAGE and stained with anti-Flag or HA Abs. Co-immunoprecipitation was confirmed with fgTICAM-1 and fgTLR22 or fgTLR3 (Fig. 5*C*), suggesting that fgTICAM-1 binds fgTLR22 and fgTLR3 in HEK cells.

Stimulation-induced recruitment of fgTICAM to fgTLR3 and fgTLR22

On cytological analyses with OLHd-rRe3 cells, overexpressed fgTICAM-1 was uniformly distributed over the cytoplasm without stimulation. The localization profile of fgTICAM-1was not much changed after poly(I:C) stimulation in later time points (Fig. 6). Likewise, a major population of fgTLR22 barely changed its localization even when stimulated with poly(I:C) (Fig. 6*B*). Only a small population appeared inside the cells in response to poly(I:C) and it partially merged with fgTICAM-1 (Fig. 6*B*). FgTLR3 was distributed in the cytoplasm in resting cells, but 2 h after the stimulation the fgTLR3 gathered to form "speckles" in the cytoplasm (Fig. 6*A*). Although some fgTLR22 and fgTLR3 colocalized with fgTICAM-1 on poly(I:C) stimulation, they gradually dissociated (Fig. 6). These data show that both fgTLR22 and fgTLR3 use TICAM-1 as the shuttling adaptor for IFN induction.

TLR22-mediated antiviral response in fish cells

Type I IFN is crucial for the antiviral response in mammals. Because fgTLR22 induced IFN in fish cells, we expected it to be required for cell protection against virus infection. To test this hypothesis, we prepared dsRNA of the IPNV (38, 39). IPNV genomic dsRNA was extracted from IPNV-infected RTG-2 cells. Isolated dsRNA of IPNV was poured over RTG-2 cells expressing fgTLR22. Like synthetic dsRNA or rotavirus-derived dsRNA (SA11), dsRNA of IPNV-induced endogenous IFN gene expression in fgTLR22-expressing cells compared with control vector-transfected cells (no induction of IFN) 2 h after stimulation (Fig. 7).

To test the resistance of RTG-2 cells to IPNV infection, we propagated a large-scale IPNV preparation amplified with RTG-2 cells. The preparation usually contained naked RNA of the IPNV genome. Thus, we prepared two infection sources for the assay: an IPNV preparation containing dsRNA, and an IPNV preparation depleted of free dsRNA. The latter sample was prepared by treating the IPNV preparation with RNase III (Fig. 8*A*). The IPNV preparations depleted of dsRNA infected RTG-2 cells and induced

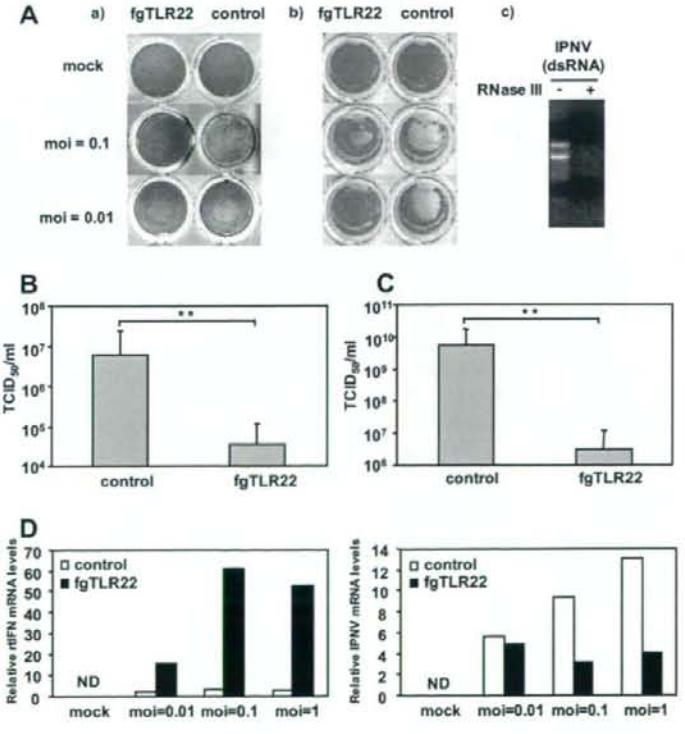

FIGURE 8. fgTLR22 expression protects cells from IPNV infection. *A*, RTG-2 cells were transfected with pEFBOS (fgTLR22) plasmid or empty vector, and 24 h later cells were exposed to the indicated moi of IPNV propagated with the RTG-2 cells. Intact IPNV (*a*) or a preparation pretreated with RNase III to remove contaminating dsRNA (*b*) was used as a virus source. dsRNA degradation was confirmed with agarose gel (*c*). At timed intervals (usually 7 days), when cells die by IPNV-induced cell death, CPE was observed under the microscope. Cells were fixed with 10% formaldehyde and stained with crystal violet. *B* and *C*, RTG-2 cells either transfected with mock or pEFBOS (fgTLR22) were infected with intact (*B*) or RNase-treated (*C*) IPNV (moi = 0.1). The medium was exchanged for removal of nonadherent viruses. Twenty-four hours after cells were replated, the supernatant was recovered and the titer checked by $TCID_{50}$. *D*, RTG-2 cells were transfected with pEFBOS (fgTLR22) or empty pEFBOS. Twenty-four hours later, cells were incubated with IPNV (moi = 0.01, 0.1, 1) for the indicated periods. After 24 h, the mRNA levels of rtIFN or IPNV were measured by quantitative PCR. Relative fold induction against the rtβ-actin level is shown. The experiments were performed three times and representative results are shown.

CPE followed by apoptosis (Fig. 8*A*). Infected RTG-2 cells were rescued from CPE if the cells expressed fgTLR22 beforehand (see the wells of moi of 0.01) (Fig. 8*A*).

We then quantitatively determined fgTLR22-mediated inhibition of IPNV infection. IPNV (moi = 0.1) (10 μg/ml) with (Fig. 8*B*) or without (Fig. 8*C*) naked dsRNA was added to TLR22-expressing RTG-2 cells. We measured the virus titer ($TCID_{50}$/ml) in the supernatants of control and fgTLR22-expressing cells. Twenty-four hours after infection, the IPNV titer was greatly decreased in fgTLR22-expressing cells compared with untransfected cells (Fig. 8, *B* and *C*). The IFN message was efficiently induced in cells with fgTLR22 concomitant with IPNV infection. Control cells, however, barely raise the IFN message in response to IPNV (Fig. 8*D*), suggesting that fgTLR22 has a critical role in IFN-mediated antiviral defense in fish cells. In conclusion, fgTLR22 governs antiviral response to a dsRNA virus IPNV via induction of fish IFN.

Discussion

Herein, we demonstrated that TLR22 is a dsRNA recognition receptor. Since fish possess both TLR3 and TLR22, they have a dual dsRNA recognition system. TLR3 and TLR22 recruit a common adaptor, TICAM-1. TLR22 preferentially recognizes long-sized dsRNA, localizes to the cell surface, and is widely distributed to tissue/organs (20). This is the first study to reveal that the TICAM-1 pathway serves as a key alert for an RNA virus sensor on the vertebrates.

According to bootstrap probability analysis, TLR22 does not belong to the TLR3 family; instead, it is proximal to mouse TLR13, which has not been characterized as a dsRNA-recognizing TLR. Thus, two arms of the TICAM-1 pathway have evolved as dsRNA receptors in fish, and only one (TLR3) has been preserved in mammals. Development of TLR22 instead of TLR3 may have some merit for protection against viruses with dsRNAs by augmenting the susceptibility of the local IFN response to long RNA duplexes in the vertebrates.

We wanted to clarify why teleosts need a cell surface RNA recognition system. Fish live in water and are exposed to many kinds of negative-stranded RNA viruses belonging to the Rhabdoviridae and to dsRNA viruses (40, 41). Bacteria such as *Rhodovulum sulfidophilum* and perhaps other species extracellularly liberate ribosomal and transfer RNAs (42). Thus, the sea may contain RNA viruses and RNA products of microbial origin. The sea is home to a unique and mysterious microbial environment. During evolution, vertebrates in water may have been protected from these pathogens by developing the set of RNA-sensing TLRs and the IFN system, which are distinct from those expressed in land animals. Our results indicate that RNA-sensing by TLRs protects fish from spreading or exacerbating infection. Viral RNAs often form a stem-loop or duplex signature (43) and are released from infected individual fish into the sea. TLR22 may sense such floating RNA as an infection threat.

Overexpressed teleost TLR22 protects host cells from infection with IPNV, which is a naked bisegmented dsRNA virus belonging to the family Birnaviridae (44). Birnaviruses have a single T = 13 icosahedral shell composed of 120 subunits and they lack the characteristic inner capsid. Aquatic birnaviruses are distributed worldwide, can infect a range of fish and shellfish species (44, 45), and are viral pathogens that cause problems in fry and young fish. Although teleosts have the gene encoding a putative ortholog of the cytoplasmic RNA sensor MDA5 (24), IPNV efficiently infect teleost cells unless TLR22 is expressed in some population of cells. Thus, fish MDA5 is insufficient for protection against this type of dsRNA virus. Although not all cells express TLR22, IFN seems to be sufficiently induced by TLR22-expressing cells (Fig. 8*D*) to provide antiviral environment in surrounding cells, resulting in host cell protection. However, how TLR22 detects the IPNV infection remains to be clarified. The necessity of TLR22 and the mode of its dsRNA recognition in fish are of interest for further investigation.

A notable difference between fgTLR22 and surface-expressed human TLR3 is that fgTLR22 is ubiquitous whereas surface TLR3 is expressed exclusively together with endosomal/ER TLR3 in TLR3-positive cells. In humans, cell-surface TLR3 is therefore distributed limitedly to the fibroblasts and epithelial cells. We previously found human TLR3 on the cell surface of fibroblasts, which therefore binds anti-TLR3 mAb, TLR3.7 (46). TLR3 on the fibroblasts recognizes exogenously added poly(I:C) to confer IFN-β induction (46). The IFN-inducing properties of human TLR3 by fibroblasts are blocked by this mAb. The result is a unique and exceptional TLR3 feature that reflects a differential TLR3 function (10). Ultimately, in humans TLR3 is expressed in the cytoplasmic compartments and on the surface of fibroblasts (33). Other reports also found that human bronchial, bile duct, and intestinal epithelial cells express TLR3 on the cell-surface membrane (47–50). In this view, surface-expressed human TLR3 is a functional remnant of fish TLR22: TLR3 functions in the mucosal region wherein body fluids are continuously in contact with the flora. Because the cell surface-associated dsRNA recognition is important even in humans, TLR3 is expressed on human fibroblasts and epithelial cells (50–52).

In this study, we found that fgTLR3 and fgTLR22 recognize its ligand dsRNA at the different sites and recruit fgTICAM-1. Although TLR22 expression is limited to part of the cell surface, a colocalization study with cholera toxin did not support its expression being restricted to lipid rafts (data not shown). Unlike the case of human TLR3, the chloroquin treatment of HEK293 cells expressing TLR22 did not abrogate the activation of the IFN-β reporter gene by poly(I:C) (data not shown). Thus, it is unlikely that TLR22 captures poly(I:C) at the endosome, as does TLR3. Human and mouse TLR3 in myeloid dendritic cells have a role in driving the cells to a maturation stage sufficiently activating NK and T cells (9, 53). It is intriguing whether TLR22 possesses this function in dendritic cells.

In this context, the question is how TLR22 assembles TICAM-1 to transmit the dsRNA-recognition signal. Possible answers may lie in the fish-specific TLR22 pathway and in the functional difference between mammalian and teleost TICAM-1. A recent study of zfTICAM-1 suggested that overexpression of zfTICAM-1 activates the zfIFN promoter but that TICAM-1 does not interact with zfTRAF6 (30). The zfTICAM-1 N-terminal region does not contain a TRAF6-binding motif, and the C-terminal region of zfTICAM-1 sufficiently activates the IFN promoter, suggesting the involvement of RIP1-mediated NF-κB activation in zfIFN promoter activation (30). In OLHd-rRe3 cells, a zebrafish minimal Mx promoter that contains two ISRE barely responds to overexpressed fgTICAM-1 or its N-terminal-deleted form, but it enhances activation of the zfIFN promoter, as shown by reporter assay. In human TICAM-1, the N-terminal region is mandatory for IRF-3-mediated type I IFN induction in the human system (14, 54). Ultimately, fish TICAM-1 behaves like human TICAM-1, although fish TICAM-1 does not mediate IRF-3 for activation of the IFN-β promoter (30). It takes a longer period for fish cells (compared with human cells; see Refs. 54, 55) to evoke TLR-TICAM-1 interaction in response to poly(I:C), which may be attributable to the temperature (~20°C) where the fish cells are grown, rather than to the difference of signaling mode. Hence, the TICAM-1 pathway is conserved across fish and humans, but its molecular

bases for IFN induction are different between them. Our speculation is that fish cells have an IFN output similar to that of human cells (54, 55) but that the signal cascade for IFN production is modally different. Teleost TICAM-1, which is partly dissimilar to human TICAM-1 in its structure, might explain the differential selection of their signal pathways.

An alternative possibility is that the IFN-inducing capacity due to the recruitment of TICAM-1 lies within the molecular feature of TLR22. Supporting evidence is that surface-expressed TLR22 retains the capacity to confer the responsiveness to poly(I:C) not only in fish RTG-2 cells but also in human HEK293 cells. FgTLR22 and even only the TIR domain of fgTLR22 can couple with human TICAM-1 as well as fish TICAM-1 to activate the human and fish ISRE promoter. Either way, TLR3 is not the only partner of TICAM-1 in the water vertebrates.

Acknowledgments

We are grateful to Drs. A. Ishii, M. Shingai, M. Sasai, K. Funami, and T. Ebihara in our laboratory for their critical discussions. Thanks are also due to Drs. T. Fujita (Kyoto Univiversity, Kyoto), T. Taniguchi (Tokyo Univiversity, Tokyo), and T. Maniatis (Harvard University, Boston, MA) for providing their plasmids.

Disclosures

The authors have no financial conflicts of interest.

References

1. Akira, S., S. Uematsu, and O. Takeuchi. 2006. Pathogen recognition and innate immunity. *Cell* 124: 783–797.
2. Honda, K., A. Takaoka, and T. Taniguchi. 2006. Type I interferon gene induction by the interferon regulatory factor family of transcription factors. *Immunity* 25: 349–360.
3. Samuel, C. E. 2001. Antiviral actions of interferons. *Clin. Microbiol. Rev.* 14: 778–809.
4. Iwasaki, A., and R. Medzhitov. 2004. Toll-like receptor control of the adaptive immune responses. *Nat. Immunol.* 5: 987–995.
5. Yoneyama, M., and T. Fujita. 2007. Function of RIG-I-like receptors in antiviral innate immunity. *J. Biol. Chem.* 28: 15315–15318.
6. Hornung, V., J. Ellegast, S. Kim, K. Brzozka, A. Jung, H. Kato, H. Poeck, S. Akira, K. K. Conzelmann, M. Schlee, et al. 2006. 5′-Triphosphate RNA is the ligand for RIG-I. *Science* 314: 994–997.
7. Pichlmair, A., O. Schulz, C. P. Tan, T. I. Naslund, P. Liljestrom, F. Weber, and C. Reis e Sousa. 2006. RIG-I-mediated antiviral responses to single-stranded RNA bearing 5′-phosphates. *Science* 314: 997–1001.
8. Kato, H., O. Takeuchi, S. Sato, M. Yoneyama, M. Yamamoto, K. Matsui, S. Uematsu, A. Jung, T. Kawai, K. J. Ishii, et al. 2006. Differential roles of MDA5 and RIG-I helicases in the recognition of RNA viruses. *Nature* 441: 101–105.
9. Matsumoto, M., and T. Seya. 2008. TLR3 signaling inducing IFN in response to dsRNA and polyI:C. *Adv. Drug Delivery Rev.* 60: 805–812.
10. Matsumoto, M., K. Funami, M. Tanabe, H. Oshiumi, M. Shingai, Y. Seto, A. Yamamoto, and T. Seya. 2003. Subcellular localization of Toll-like receptor 3 in human dendritic cells. *J. Immunol.* 171: 3154–3162.
11. Oganesyan, G., S. K. Saha, B. Guo, J. Q. He, A. Shahangia, B. Zarnegar, A. Perry, and G. Cheng. 2006. Critical role of TRAF3 in the Toll-like receptor-dependent and-independent antiviral response. *Nature* 439: 208–211.
12. Hacker, H., V. Redecke, B. Blagoev, I. Kratchmarova, L. C. Hsu, G. G. Wang, M. P. Kamps, E. Raz, H. Wagner, G. Hacker, et al. 2006. Specificity in Toll-like receptor signalling through distinct effector functions of TRAF3 and TRAF6. *Nature* 439: 204–207.
13. Ryzhakov, G., and F. Randow. 2007. SINTBAD, a novel component of innate antiviral immunity, shares a TBK1-binding domain with NAP1 and TANK. *EMBO J.* 26: 3180–3190.
14. Sasai, M., H. Oshiumi, M. Matsumoto, N. Inoue, F. Fujita, M. Nakanishi, and T. Seya. 2005. Cutting edge: NF-κB-activating kinase-associated protein 1 participates in TLR3/Toll-IL-1 homology domain-containing adapter molecule-1-mediated IFN regulatory factor 3 activation. *J. Immunol.* 174: 27–30.
15. Sasai, M., M. Shingai, K. Funami, M. Yoneyama, T. Fujita, M. Matsumoto, and T. Seya. 2006. NAK-associated protein 1 participates in both the TLR3 and the cytoplasmic pathways in type I IFN induction. *J. Immunol.* 177: 8676–8683.
16. Hoebe, K., X. Du, P. Georgel, E. Janssen, K. Tabeta, S. O. Kim, J. Goode, P. Lin, N. Mann, S. Mudd, et al. 2003. Identification of Lps2 as a key transducer of MyD88-independent TIR signalling. *Nature* 424: 743–748.
17. Stack, J., I. R. Haga, M. Schroder, N. W. Bartlett, G. Maloney, P. C. Reading, K. A. Fitzgerald, G. L. Smith, and A. G. Bowie. 2005. Vaccinia virus protein A46R targets multiple Toll-like-interleukin-1 receptor adaptors and contributes to virulence. *J. Exp. Med.* 201: 1007–1018.
18. Altmann, S. M., M. T. Mellon, D. L. Distel, and C. H. Kim. 2003. Molecular and functional analysis of an interferon gene from the zebrafish, *Danio rerio*. *J. Virol.* 77: 1992–2002.
19. Robertsen, B. 2006. The interferon system of teleost fish. *Fish Shellfish Immunol.* 20: 172–191.
20. Oshiumi, H., T. Tsujita, K. Shida, M. Matsumoto, K. Ikeo, and T. Seya. 2003. Prediction of the prototype of the human Toll-like receptor gene family from the pufferfish, *Fugu rubripes*, genome. *Immunogenetics* 54: 791–800.
21. Roach, J. C., G. Glusman, L. Rowen, A. Kaur, M. K. Purcell, K. D. Smith, L. E. Hood, and A. Aderem. 2005. The evolution of vertebrate Toll-like receptors. *Proc. Natl. Acad. Sci. USA* 102: 9577–9582.
22. Meijer, A. H., S. F. Gabby Krens, I. A. Medina Rodriguez, S. He, W. Bitter, B. Ewa Snaar-Jagalska, and H. P. Spaink. 2004. Expression analysis of the Toll-like receptor and TIR domain adaptor families of zebrafish. *Mol. Immunol.* 40: 773–783.
23. Jault, C., L. Pichon, and J. Chluba. 2004. Toll-like receptor gene family and TIR-domain adapters in *Danio rerio*. *Mol. Immunol.* 40: 759–771.
24. Ishii, A., M. Kawasaki, M. Matsumoto, S. Tochinai, and T. Seya. 2007. Phylogenetic and expression analysis of amphibian *Xenopus* Toll-like receptors. *Immunogenetics* 59: 281–293.
25. Oshiumi, H., M. Matsumoto, K. Funami, T. Akazawa, and T. Seya. 2003. TICAM-1, an adapter molecule that participates in Toll-like receptor 3-mediated interferon-β induction. *Nat. Immunol.* 4: 161–167.
26. Tsujita, T., H. Tsukada, M. Nakao, H. Oshiumi, M. Matsumoto, and T. Seya. 2004. Sensing bacterial flagellin by membrane and soluble orthologs of Toll-like receptor 5 in rainbow trout (*Onchorhynchus mikiss*). *J. Biol. Chem.* 279: 48588–48597.
27. Higuchi, M., A. Matsuo, M. Shingai, K. Shida, A. Ishii, K. Funami, Y. Suzuki, H. Oshiumi, M. Matsumoto, and T. Seya. 2007. Combinational recognition of bacterial lipoproteins and peptidoglycan by chicken Toll-like receptor 2 subfamily. *Dev. Comp. Immunol.* 32: 147–155.
28. Medzhitov, R., P. Preston-Hurlburt, and C. A. Janeway, Jr. 1997. A human homologue of the *Drosophila* Toll protein signals activation of adaptive immunity. *Nature* 388: 394–397.
29. Okahira, S., F. Nishikawa, S. Nishikawa, T. Akazawa, T. Seya, and M. Matsumoto. 2005. Interferon-β induction through Toll-like receptor 3 depends on double-stranded RNA structure. *DNA Cell Biol.* 24: 614–623.
30. Sullivan, C., J. H. Postlethwait, C. R. Lage, P. J. Millard, and C. H. Kim. 2007. Evidence for evolving Toll-IL-1 receptor-containing adaptor molecule function in vertebrates. *J. Immunol.* 178: 4517–4527.
31. Jensen, I., A. Albuquerque, A. I. Sommer, and B. Robertsen. 2002. Effect of polyI:C on the expression of Mx proteins and resistance against infection by infectious salmon anaemia virus in Atlantic salmon. *Fish Shellfish Immunol.* 13: 311–326.
32. Carty, M., R. Goodbody, M. Schroder, J. Stack, P. N. Moynagh, and A. G. Bowie. 2006. The human adaptor SARM negatively regulates adaptor protein TRIF-dependent Toll-like receptor signaling. *Nat. Immunol.* 7: 1074–1081.
33. Funami, K., M. Matsumoto, H. Oshiumi, T. Akazawa, A. Yamamoto, and T. Seya. 2004. The cytoplasmic "linker region" in Toll-like receptor 3 controls receptor localization and signaling. *Int. Immunol.* 16: 1143–1154.
34. Nishiya, T., E. Kajita, S. Miwa, and A. L. Defranco. 2005. TLR3 and TLR7 are targeted to the same intracellular compartments by distinct regulatory elements. *J. Biol. Chem.* 280: 37107–37117.
35. Latz, E., A. Schoenemeyer, A. Visintin, K. A. Fitzgerald, B. G. Monks, C. F. Knetter, E. Lien, N. J. Nilsen, T. Espevik, and D. T. Golenbock. 2004. TLR9 signals after translocating from the ER to CpG DNA in the lysosome. *Nat. Immunol.* 5: 190–198.
36. Hirayama, M., H. Mitani, and S. Watabe. 2006. Temperature-dependent growth rates and gene expression patterns of various medaka *Oryzias latipes* cell lines derived from different populations. *J. Comp. Physiol. B* 176: 311–320.
37. Purcell, M. K., K. D. Smith, L. Hood, J. R. Winton, and J. C. Roach. 2006. Conservation of Toll-like receptor signaling pathways in teleost fish. *Comp. Biochem. Physiol. D Genomics Proteomics* 1: 77–88.
38. Jensen, V., and B. Robertsen. 2000. Cloning of an Mx cDNA from Atlantic halibut (*Hippoglossus hippoglossus*) and characterization of Mx mRNA expression in response to double-stranded RNA or infectious pancreatic necrosis virus. *J. Interferon Cytokine Res.* 20: 701–710.
39. Collet, B., E. S. Munro, S. Gahlawat, F. Acosta, J. Garcia, C. Roemelt, J. Zou, C. J. Secombes, and A. E. Ellis. 2007. Infectious pancreatic necrosis virus suppresses type I interferon signalling in rainbow trout gonad cell line but not in Atlantic salmon macrophages. *Fish Shellfish Immunol.* 22: 44–56.
40. Phelan, P. E., M. E. Pressley, P. E. Witten, M. T. Mellon, S. Blake, and C. H. Kim. 2005. Characterization of snakehead rhabdovirus infection in zebrafish (*Danio rerio*). *J. Virol.* 79: 1842–1852.
41. Nishizawa, T., S. Kinoshita, and M. Yoshimizu. 2005. An approach for genogrouping of Japanese isolates of aquabirnaviruses in a new genogroup, VII, based on the VP2/NS junction region. *J. Gen. Virol.* 86: 1973–1978.
42. Ando, T., H. Suzuki, S. Nishimura, T. Tanaka, A. Hiraishi, and K. Kikuchi. 2006. Characterization of extracellular RNAs produced by the marine photosynthetic bacterium *Rhodovulum sulfidophilum*. *J. Biochem.* 139: 805–811.
43. Shingai, M., T. Ebihara, N. A. Begum, A. Kato, T. Honma, K. Matsumoto, H. Saito, H. Ogura, M. Matsumoto, and T Seya. 2007. Differential type I interferon (IFN) inducing abilities of wild-type vs. vaccine strains of measles virus. *J. Immunol.* 179: 6123–6133.
44. Coulibaly, F., C. Chevalier, I. Gutsche, J. Pous, J. Navaza, S. Bressanelli, B. Delmas, and F. A. Rey. 2005. The birnavirus crystal structure reveals structural relationships among icosahedral viruses. *Cell* 120: 761–772.
45. Jensen, I., and B. Robertsen. 2002. Effect of double-stranded RNA and interferon on the antiviral activity of Atlantic salmon cells against infectious salmon anemia

virus and infectious pancreatic necrosis virus. *Fish Shellfish Immunol.* 13: 221–241.
46. Matsumoto, M., S. Kikkawa, M. Kohase, K. Miyake, and T. Seya. 2002. Establishment of a monoclonal antibody against human Toll-like receptor 3 that blocks double-stranded RNA-mediated signaling. *Biochem. Biophys. Res. Commun.* 293: 1364–1369.
47. Rudd, B. D., J. J. Smit, R. A. Flavell, L. Alexopoulou, M. A. Schaller, A. Gruber, A. A. Berlin, and N. W. Lukacs. 2006. Deletion of TLR3 alters the pulmonary immune environment and mucus production during respiratory syncytial virus infection. *J. Immunol.* 176: 1937–1942.
48. Liu, P., M. Jamaluddin, K. Li, R. P. Garofalo, A. Casola, and A. R. Brasier. 2007. Retinoic acid-inducible gene I mediates early antiviral response and Toll-like receptor 3 expression in respiratory syncytial virus-infected airway epithelial cells. *J. Virol.* 81: 1401–1411.
49. Cario, E., and D. K. Podolsky. 2000. Differential alteration in intestinal epithelial cell expression of Toll-like receptor 3 (TLR3) and TLR4 in inflammatory bowel disease. *Infect. Immun.* 68: 7010–7017.
50. Nakamura, M., K. Funami, A. Komori, T. Yokoyama, Y. Aiba, A. Araki, Y. Takii, M. Ito, M. Matsuyama, M. Koyabu, et al. 2008. Increased expression of TLR3 in human intrahepatic biliary epithelial cells at the site of ductular reaction in primary billiary cirrhosis. *Hepatol. Intern.* In press.
51. Harada, K., Y. Sato, K. Itatsu, K. Isse, H. Ikeda, M. Yasoshima, Y. Zen, A. Matsui, and Y. Nakanuma. 2007. Innate immune response to double-stranded RNA in biliary epithelial cells is associated with the pathogenesis of biliary atresia. *Hepatology* 46: 1146–1154.
52. Zhou, R., H. Wei, R. Sun, and Z. Tian. 2007. Recognition of double-stranded RNA by TLR3 induces severe small intestinal injury in mice. *J. Immunol.* 178: 4548–4556.
53. Ebihara, T., M. Shingai, M. Matsumoto, K. Shimotohno, T. Wakita, and T. Seya. 2008. Hepatitis C virus (HCV)-infected apoptotic cells extrinsically modulate dendritic cell function to activate T cells and NK cells. *Hepatology.* 48: 48–58.
54. Funami, K., M. Sasai, Y. Ohba, H. Oshiumi, T. Seya, and M. Matsumoto. 2007. Spatiotemporal mobilization of TICAM-1 in response to dsRNA. *J. Immunol.* 179: 6827–6830.
55. Funami, K., M. Sasai, H. Oshiumi, T. Seya, and M. Matsumoto. 2008. Homo-oligomerization is essential for Toll/IL-1 receptor domain containing adaptor molecule-1 signaling. *J. Biol. Chem.* 283: 18283–18291.

Hepatitis C Virus–Infected Hepatocytes Extrinsically Modulate Dendritic Cell Maturation To Activate T Cells and Natural Killer Cells

Takashi Ebihara,[1] Masashi Shingai,[1] Misako Matsumoto,[1] Takaji Wakita,[2] and Tsukasa Seya[1]

Dendritic cell maturation critically modulates antiviral immune responses, and facilitates viral clearance. Hepatitis C virus (HCV) is characterized by its high predisposition to persistent infection. Here, we examined the immune response of human monocyte-derived dendritic cells (MoDCs) to the JFH1 strain of HCV, which can efficiently replicate in cell culture. However, neither HCV RNA replication nor antigen production was detected in MoDCs inoculated with JFH1. None of the indicators of HCV interacting with MoDCs we evaluated were affected, including expression of maturation markers (CD80, 83, 86), cytokines (interleukin-6 and interferon-beta), the mixed lymphocyte reaction, and natural killer (NK) cell cytotoxicity. Strikingly, MoDCs matured by phagocytosing extrinsically-infected vesicles containing HCV-derived double-stranded RNA (dsRNA). When MoDCs were cocultured with HCV-infected apoptotic Huh7.5.1 hepatic cells, there was increased CD86 expression and interleukin-6 and interferon-beta production in MoDCs, which were characterized by the potential to activate NK cells and induce $CD4^+$ T cells into the T helper 1 type. Lipid raft-dependent phagocytosis of HCV-infected apoptotic vesicles containing dsRNA was indispensable to MoDC maturation. Colocalization of dsRNA with Toll-like receptor 3 (TLR3) in phagosomes suggested the importance of TLR3 signaling in the MoDC response against HCV. *Conclusion:* The JFH1 strain does not directly stimulate MoDCs to activate T cells and NK cells, but phagocytosing HCV-infected apoptotic cells and their interaction with the TLR3 pathway in MoDCs plays a critical role in MoDC maturation and reciprocal activation of T and NK cells. (HEPATOLOGY 2008;48:48-58.)

Abbreviations: CPZ, chlorpromazine; CTL, cytotoxic T lymphocyte; DC, dendritic cell; DC-SIGN, dendritic cell-specific intercellular adhesion molecule 3-grabbing nonintegrin; dsRNA, double-stranded RNA; ELISA, enzyme-linked immunosorbent assay; FACS, fluorescence-activated cell sorting; HCV, hepatitis C virus; IFN, interferon; IFNAR, type I IFN-alpha receptor; IL, interleukin; IRF, IFN regulatory factor; MβCD, methyl-beta-cyclodextrin; MDA5, melanoma differentiation associated gene 5; mAb, monoclonal antibody; MoDC, monocyte-derived dendritic cell; MOI, multiplicity of infection; MV, measles virus; NK, natural killer; NKG2D, natural killer group 2, member D; PAMP, pathogen associated molecular pattern; PBMC, peripheral blood mononuclear cells; pDC, plasmacytoid DC; poly I:C, polyinosinic:polycytidylic acid; RIG-I, retinoic acid inducible gene I; RSV, respiratory syncytial virus; RT-PCR, reverse-transcription polymerase chain reaction; siRNA, small interfering RNA; SNARF1, far red immunofluorescence dye; Th1, T helper 1; TLR, Toll-like receptor; TNF, tumor necrosis factor.

From the [1]Department of Microbiology and Immunology, Hokkaido University Graduate School of Medicine, Sapporo, Japan; and [2]Department of Virology II, National Institute of Infectious Diseases, Tokyo, Japan.

Received September 10, 2007; accepted March 11, 2008.

Supported in part by CREST and Innovation, Japan Science and Technology Corporation, the Program of Founding Research Centers for Emerging and Reemerging Infectious Diseases, MEXT, and Grants-in-Aid from the Ministry of Education, Science, and Culture (Specified Project for Advanced Research) and the Ministry of Health, Labor, and Welfare of Japan and the HCV project in National Institute of Health of Japan, and by the Takeda Foundation, Uehara memorial Foundation, Mitsubishi Foundation, Akiyama Foundation, and NorthTec Foundation.

Masashi Shingai is currently affiliated with the Laboratory of Molecular Microbiology, National Institute of Allergy and Infectious Diseases, National Institutes of Health, Bethesda, MD.

Address reprint requests to: Tsukasa Seya, Department of Microbiology and Immunology, Graduate School of Medicine, Hokkaido University, Kita-ku, Sapporo, 060-8638, Japan. E-mail: seya-tu@pop.med.hokudai.ac.jp; fax: 81-11-706-7866.

Published online in Wiley InterScience (www.interscience.wiley.com).

DOI 10.1002/hep.22337

Potential conflict of interest: Nothing to report.

Hepatitis C virus (HCV) is a single-strand, positive-sense RNA virus belonging to the flaviviridae family. HCV develops persistent infection in <70% of infected patients, and eventually causes chronic hepatitis, cirrhosis, and hepatocellular carcinoma in some patients.[1] Once chronic infection is established in patients with HCV, spontaneous viral clearance fails,[1] although how HCV remains persistently infecting the liver is unknown. It has been accepted that successful viral clearance by the host is largely attributed to robust induction of type I interferon (IFN) and antiviral cellular effectors, cytotoxic T lymphocyte (CTL) and natural killer (NK) cells.[2-5] In HCV-infected patients and chimpanzees, type I IFN induction and activation of HCV-specific $CD4^+$ T/$CD8^+$ T cells and NK cells are indeed detected during acute infection.[4-6] However, why these antiviral factors cannot eradicate HCV from most patients is not addressed. Facilities for inducing the antiviral effectors and their role against HCV persistence have not been well determined. A main cause for the deficiency of knowledge on the host response to HCV is the lack of an appropriate model for experimental HCV infection.

Two breakthroughs have now made it possible to investigate the immune response against HCV. First, Toll-like receptors (TLRs) and other innate immune receptors of dendritic cells (DCs) were found to be involved in the host antiviral IFN response, followed by CTL and NK cell activation.[2,7-9] Some reports revealed that HCV proteins participate in the regulation of IFN-inducing innate responses.[10-12] Second, an *in vitro* amplifiable 2a type HCV strain, JFH1, was established by Wakita et al.[13] and Zhong et al.[14] Infection studies for testing HCV replication and the immune response are therefore now feasible *in vitro*.

There are two major subsets of DCs in humans: plasmacytoid DCs (pDCs) expressing TLR7 and TLR9 and myeloid DCs expressing Toll-like receptor 3 (TLR3) for viral RNA/DNA recognition. Cytoplasmic RNA sensors, retinoic acid inducible gene I (RIG-I)-like receptors, also participate in viral RNA recognition and IFN induction.[7] RNA virus infection allows pDCs to induce type I IFN via TLR7.[15] On the contrary, myeloid DCs recognize virus-derived double-stranded RNA (dsRNA) to activate pathways for IFN-beta production and NK/CTL induction.[7-9,16] What happens in the pathway of myeloid DC maturation during HCV infection can now be experimentally followed up in infected cells as the JFH1 strain can be used for *in vitro* infection studies. Hence, we inoculated monocyte-derived (Mo)DCs with JFH1 of HCV.

Here, we show evidence that the JFH1 strain has no direct route for MoDC infection and MoDCs phagocytosing HCV-infected apoptotic vesicles participate in MoDC maturation and reciprocal activation of T cells and NK cells.

Materials and Methods

Cell Lines, Antibodies, and Reagents. Huh7.5.1 cells were kindly provided by Dr. Francis V. Chisari (The Scripps Research Institute, La Jolla, CA), and maintained in Dulbecco's modified Eagle's medium–based medium.[14] Following materials were obtained as indicated: anti-HCV-core monoclonal antibody (mAb; C7-50) from Affinity BioReagents (Golden, CO), mAbs against CD80, CD83, and CD86 from Immunotech (Fullerton, CA), anti-dsRNA mAb (K1) from English & Scientific Consulting Bt (Szirak, Hungary), biotin-conjugated anti-TLR3 mAb from eBioscience (San Diego, CA), fluorescein isothiocyanate–labeled goat anti-mouse immunoglobulin G from American Qualex (San Clemente, CA), Streptavidin Alexa Fluor 594 conjugate and SNARF1 from Molecular Probe (Carlsbad, CA), Methyl-beta-cyclodextrin (MβCD), chlorpromazine (CPZ), and bafilomycin (BAF) from Sigma-Aldrich (St. Louis, MO).

Preparation of Immature MoDCs, NK Cells, and T Cells. $CD14^+$ monocytes and autologous NK cells were isolated from human peripheral blood mononuclear cells (PBMCs) using a MACS system (Miltenyi Biotec, Bergisch Gladbach, Germany).[17] Cells purified by this technique had an average purity of 95%, as assessed by flow cytometry. Immature MoDCs were generated from monocytes using human granulocyte-macrophage colony-stimulating factor (GM-CSF; PeproTech, Rocky Hill, NJ) and interleukin (IL)-4 (PeproTech).[17] Autologous NK cells were stocked in Cell Banker (Diaton, Tokyo, Japan) at −80°C. Allogeneic $CD4^+$ and $CD8^+$ T cells were also negatively isolated by a MACS system (Miltenyi Biotec).

Stimulation of Immature MoDC, Cytokine Assay, Immunofluorescent Staining, and Flow Cytometry. The immature MoDCs (2×10^5) were inoculated with HCV and respiratory syncytial virus (RSV) at a multiplicity of infection (MOI) of one or treated with polyinosinic: polycytidylic acid (poly I:C; 10 μg/mL), and cultured in a 24-well plate. The cells and culture supernatant were harvested at indicated time points for reverse transcription polymerase chain reaction (RT-PCR), fluorescence-activated cell sorting (FACS), and enzyme-linked immunosorbent assay (ELISA; IFN-beta, IFN-gamma; Fujirebio, Inc., Tokyo, Japan; IL-6; BD Biosciences, Franklin Lakes, NJ). In some experiments, immature MoDCs (2×10^5) were cocultured with HCV- or non-infected apoptotic cells (4×10^5). MoDCs were treated with MβCD (1 mM), CPZ (5 μg/mL), and BAF (100

nM) for 1 hour before coculture. The viability of these MoDCs was examined by proidium iodide staining. After 2 days of coculture, the MoDCs were isolated from the apoptotic cells by Ficoll-Paque Plus (GE-Healthcare, Waukesha, WI) using the manufacturer's methods, and used for further analysis to assess MoDC functions. The cell lysates were produced from the apoptotic cells by three freeze/thaw cycles, followed by centrifugation at 15,000 rpm for 5 minutes or by sonication three times for 20 seconds on ice. Total RNA was extracted by Trizol (Invitrogen, Carlsbad, CA) by the manufacturer's methods. MoDCs (5×10^5 cells) were transfected with 0.625 μg total RNA by N-[1-(2,3-Dioleoyloxy)propyl]-N, N, N-trimethylammonium methyl-sulfate (DOTAP; Roche, Mannheim, Germany) and cultured in 24-well plates for 1 day. Huh7.5.1 cells were transfected with poly I:C using Lipofectamine 2000 (Invitrogen) by the manufacturer's methods. ELISA for determination of cytokine levels, flow cytometry, and immunofluorescent staining were performed as reported.[17,18]

Virus Propagation. The method to generate infectious HCV particles was referred to an *in vitro* system using the plasmid pJFH-1.[16] Noninfected cell supernatant was used as noninfected control. The concentrated virus had a titer of 1 to 2×10^6 ffu/mL. A RSV field-isolate strain (RSV2177) was propagated with Hep-2 cells as described.[17] The titer of RSV2177 was determined by 50% tissue culture infective dose (TCID50) with Hep-2 cells.

Real-time PCR Quantification of Positive-Strand and Negative-Strand HCV RNA. Total Trizol-extracted RNA was analyzed by reverse transcription-PCR (RT-PCR) with a modification of the previously described strand-specific rTth RT-PCR method.[19] RT primers for complementary DNA synthesis of positive and negative strand HCV RNA were GTGCACGGTCTACGAGACCT and GAGTGTCGTACAGCCTCCAG, respectively. Positive-strand and negative-strand HCV PCR amplifications were performed using Platinum SYBR Green qPCR SuperMix-UDG (Invitrogen) with 200 nM of paired primers, forward CGGGAGAGCCATAGTGG and reverse AGTACCACAAGGCCTTTCG. The PCR conditions were 95°C for 10 minutes, followed by 40 cycles of 95°C for 15 seconds and 60°C for 1 minute. This PCR method could detect 10 copies of positive-strand or negative-strand HCV.

Induction and Certification of Apoptosis. A total of 1×10^5 Huh7.5.1 cells were plated in a 24-well plate and infected with the JFH1 strain at an MOI of 1. At indicated timed intervals, the infected cells and poly I:C-transfected cells were pretreated with cycloheximide

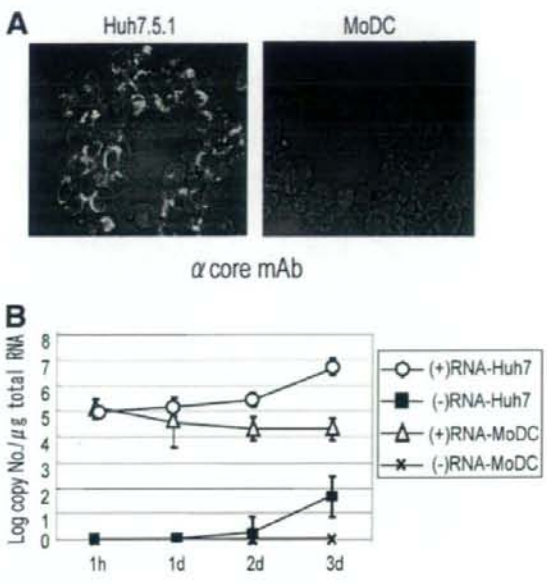

Fig. 1. MoDCs are not permissive for HCV replication. (A) Huh7.5.1 cells and MoDCs were inoculated with HCV at an MOI of 1 and cultured for 3 days. The presence of HCV core antigens was assessed by immunofluorescent staining. (B) Real-time RT-PCR to detect positive-strand and negative-strand HCV RNA. Data show means ± SD from three independent experiments using three different donors.

(20 μg/mL; Sigma) for 30 minutes, followed by tumor necrosis factor (TNF)-alpha (10 ng/mL; Pepro-Tech). The HCV-infected and noninfected apoptotic cells were harvested after another 24-hour culture. Using the HCV-infected apoptotic cells, we examined the presence of HCV core antigens and dsRNA by FACS using anti-HCV core mAb and anti-dsRNA mAb, respectively. Apoptosis was assessed by 4′,6-diamidino-2-phenylindole-staining, DNA fragmentation, and FACS by using fluorescein isothiocyanate–labeled annexin-V and proidium iodide (Roche).[20]

Assay for Lymphocyte Proliferation by MoDC. After 2 days culture of MoDCs with HCV, poly I:C (10 μg/mL), or the apoptotic cells, MoDCs were harvested and treated with mitomycin C (20 μg/mL) in phosphate buffered saline for 45 minutes. For the proliferation assay, the stimulated-MoDCs (1×10^4) were cultured with 1×10^5 allogeneic PBMCs, $CD4^+$ T cells, or $CD8^+$ T cells in U-bottom 96-well plates for 6 days. During the last 24 hours of culturing, [^{3}H]thymidine (1 mCi/well) was added to the culture medium. Then the cells and medium were harvested separately by a cell-harvester, and the radioactivity was measured by a liquid scintillation counter (Aloca, Tokyo, Japan). For the analysis of $CD4^+$ T cell polarization, the stimulated-MoDCs (1×10^4) were

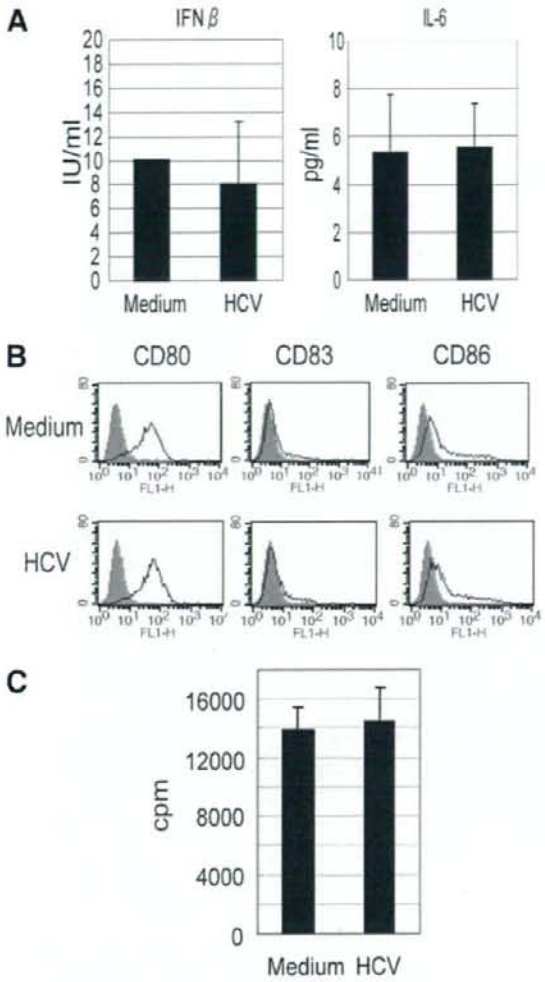

Fig. 2. HCV fails to induce MoDC maturation and cytokine response. MoDCs were inoculated with HCV at an MOI of 1 and cultured for 48 hours. (A) The supernatant was assayed for production of IFN-beta and IL-6. (B) The cells were harvested for FACS and (C) mixed lymphocyte reaction (MIR). Allogeneic PBMC were cultured with the inoculated-MoDCs for 6 days. Proliferation was determined by [^{3}H]thymidine uptake. Data show means ± SD of duplicate or triplicate samples from one experiment representative of three donors.

treated with mitomycin C and cultured with allogeneic $CD4^+$ T cells (1×10^5) for 6 days. Then the cells were washed and transferred to new round-bottom 96-well plates. Phorbol 12-myristate 13-acetate (10 ng/mL; Sigma-Aldrich) and ionomycin (1 μg/mL; Sigma-Aldrich) were added and plates were incubated for a further 24 hours. Supernatants were harvested for cytokine production (IL-4, IFN-gamma; GE-Healthcare).

MoDC-NK Coculture and ^{51}Cr Release Assay. The stimulated-MoDCs were harvested for MoDC-NK coculture at indicated time points. Autologous NK cells (5×10^5) were cocultured with the MoDCs (1×10^5) in 24-well plates for 24 hours. Transwell (Corning) was inserted to block the MoDC-NK cell contact. The supernatants and NK cells were collected from the MoDC-NK coculture and assayed for IFN-gamma production (GE Healthcare) and cytotoxicity against K562. Cytotoxicity was determined by standard ^{51}Cr release assay as described.[17]

Gene Silencing of TLR3 in MoDC. Small interfering RNA (siRNA)-based gene knockdown was preformed with MoDCs by electroporation as described.[21] siRNA duplexes (small interfering TLR3: cat #107056, negative control: cat #AM4635) were obtained from Ambion (Tokyo, Japan). Expression of TLR3 was examined by SYBR green real-time PCR using forward primer, AAGACCCATTATG-CAAAAGATTCAA and reverse primer, TCCAGATTTT-GTTCAATAGCTTGTTG. MoDCs (1×10^6 cells) were electroporated with these siRNA and cultured for 4 hours. Then, HCV-infected or noninfected apoptotic Huh7.5.1

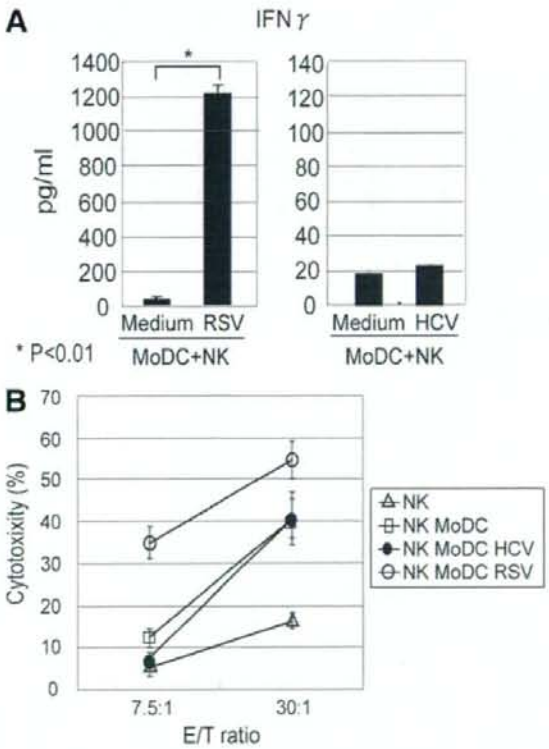

Fig. 3. MoDCs inoculated with HCV barely activate NK cells. MoDCs were harvested at 24 hours after inoculation of RSV and HCV. Autologous NK cells were cocultured with the MoDCs for 24 hours. (A) The supernatant were assayed for NK IFN-gamma production. (B) NK cells were harvested for ^{51}Cr release assay to examine NK cytotoxic activity against K562. A representative of the three similar experiments with individual donors is shown.

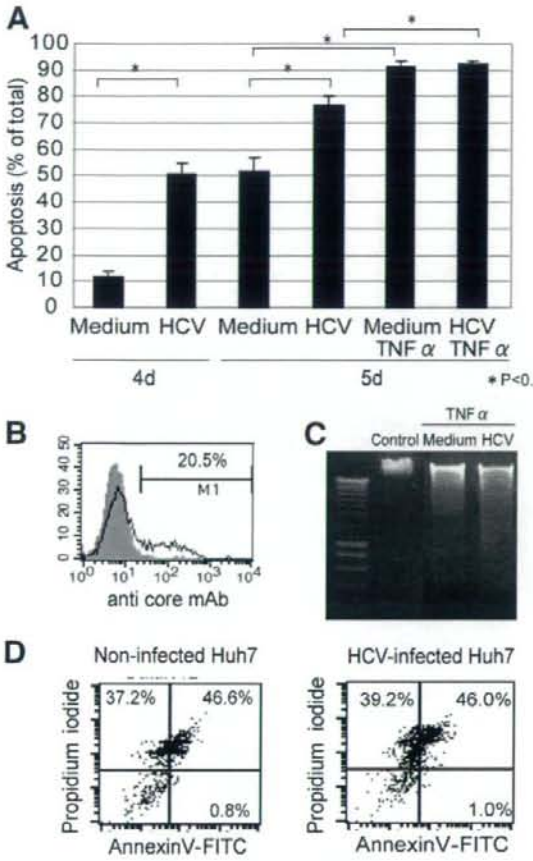

Fig. 4. Preparation of HCV-infected apoptotic Huh7.5.1 cells. Huh7.5.1 cells were infected with HCV at an MOI of 1 and culture for 4 or 5 days. Apoptosis was induced by cycloheximide and TNF-alpha after 4 days culture. At 5 days after infection, the apoptotic cells were harvested for counting 4′,6-diamidino-2-phenylindole stained apoptotic nuclei, FACS and examination of DNA fragmentation. (A) Typical apoptotic cells stained with 4′,6-diamidino-2-phenylindole were counted among <1000 cells and percent cell apoptosis was determined. Data are means ± SD from three independent experiments, each performed in triplicate. (B) HCV-core antigens were detected in the HCV-infected apoptotic cells by FACS. (C) DNA was extracted from HCV- or noninfected apoptotic Huh7.5.1 cells and electrophoresed on agarose gels to evaluate DNA fragmentation. (D) HCV- and noninfected Huh7.5.1 cells were examined for stages of apoptosis by FACS using annexin V-fluorescein isothiocyanate (FITC) and proidium iodide. Data shown are representative of three independent experiments.

cells (2×10^6 cells) were added to the wells. After 48 hours of culture, the supernatants were harvested and examined for cytokine concentrations by ELISA.

Results

MoDCs Are Not Permissive for HCV Replication. MoDCs and Huh7.5.1 cells were inoculated with the JFH1 strain at an MOI of 1, then the cells were harvested for immunofluorescent staining and sequence-specific real-time RT-PCR at indicated time points after inoculation. HCV genome RNA (negative sense of HCV RNA) was replicated in Huh7.5.1 cells but not to a detectable level in MoDCs at 2 to 3 days after inoculation (Fig. 1B). Accordingly, HCV core antigens were detected in Huh7.5.1 cells, but not in MoDCs, by immunofluorescent staining until 3 days after HCV inoculation (Fig. 1A). Similar results were obtained with monocyte-derived macrophages and BDCA4$^+$ pDCs (data not shown).

MoDC Maturation and Cytokine Response Against the JFH1 Strain. DCs work as key producers of innate inflammatory cytokines in response to pathogen-associated molecular patterns (PAMPs). However, MoDCs inoculated with JFH1 (MOI = 1) did not produce IFN-gamma or IL-6 over the noninfected control (Fig. 2A). MoDCs stimulated with PAMPs mature to up-regulate CD80/CD86 expression and activate T cells. Some reports showed that the MoDC maturation was induced following incorporation of HCV pseudotype particles into the MoDCs.[22] However, expression of costimulatory molecules (CD80, CD86) and a maturation marker (CD83) were not up-regulated by inoculation with the JFH1 strain (MOI = 1; Fig. 2B). MoDCs cocultured with JFH1 strain did not enhance the proliferation of allogeneic PBMC compared with noninoculated MoDCs (Fig. 2C).

MoDCs Exposed to the JFH1 Strain Do Not Activate NK Cells. MoDCs are known to recognize PAMPs and promote NK cell activation via MoDC/NK reciprocal interaction.[9] We have reported that NK cells are activated by MoDCs infected with RNA viruses, such as RSV, influenza virus, and measles virus.[17] We inoculated MoDCs with RSV or the JFH1 strain at an MOI of 1 and cocultured the MoDCs with autologous NK cells. After 1-day of coculture, NK cell IFN-gamma and cytotoxicity were markedly induced by RSV-treated MoDCs but not HCV-treated MoDCs (Fig. 3A,B).

HCV-Infected Apoptotic Cells Induce MoDC Maturation and Cytokine Responses. Then, we moved on to whether HCV-infected cells affect MoDC maturation. We first cocultured MoDCs with HCV-infected or noninfected Huh7.5.1 cells and examined IL-6 production by MoDCs. MoDCs cocultured with HCV-infected Huh7.5.1 cells secreted more IL-6 than those with noninfected Huh7 cells (Fig. 5A). However, since HCV infection induced apoptosis in Huh7.5.1 cells, HCV-infected and noninfected Huh7 cells were not in the same apoptotic stages (Fig. 4A). We had to exclude the possibility that apoptotic events themselves affect MoDC maturation. Therefore, we forced HCV-infected and

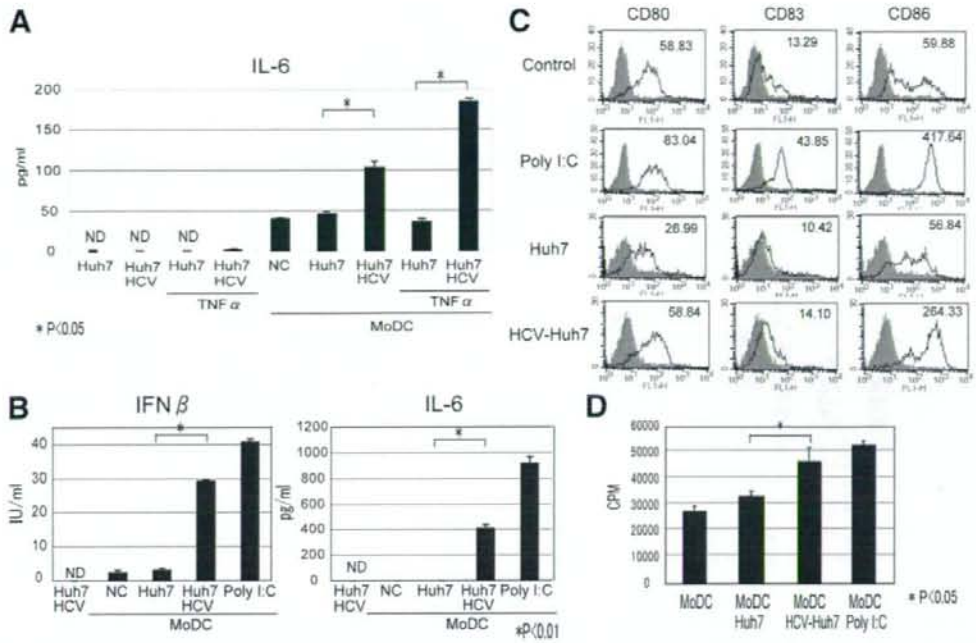

Fig. 5. HCV-infected apoptotic cells induce MoDC maturation and cytokine response. MoDCs were cocultured with HCV-infected/noninfected apoptotic or nonapoptotic cells for 2 days. Polyl:C stimulation was used as a positive control. (A,B) The culture supernatants were assayed for determination of IFN-beta and IL-6. The MoDCs were isolated from the apoptotic cells and used for (C) FACS and (D) mixed lymphocyte reaction (MLR). MoDC maturation was examined by the expression of CD80, CD83, and CD86 (C, a representative of three donor experiments). Allogeneic PBMCs were cultured with the MoDCs for 6 days. Proliferation was determined by [^{3}H]thymidine uptake (D, means ± SD of triplicate samples from one representative of three donors).

noninfected cells to induce full apoptosis by cycloheximide and TNF-alpha to the same level of apoptotic stages (Fig. 4A). HCV core antigens were detected in 20.5% of the HCV-infected apoptotic cells (Fig. 4B). Apoptotic nuclei were observed in almost all of HCV-infected and noninfected cells (Fig. 4A). DNA ladder formation, a hallmark of apoptosis, was detected in HCV-infected and noninfected apoptotic Huh7.5.1 cells to similar levels (Fig. 4C). Apoptotic cells, either infected or noninfected, gave similar profiles by flow cytometry using annexin-V for early apoptosis and propidium iodide for late apoptosis (Fig. 4D).

We applied these HCV-infected and noninfected apoptotic cells to MoDCs and determined the concentration of IFN-beta and IL-6 in the culture supernatants. HCV-infected apoptotic cells facilitated the production of IFN-beta and IL-6 by MoDCs compared with noninfected apoptotic cells (Fig. 5B). In this context, HCV products, rather than undergoing apoptosis, in infected cells are an essential factor for induction of MoDC maturation (Fig. 5A).

We next examined whether MoDC maturation was induced by HCV-infected apoptotic cells. After coculture of MoDCs with the apoptotic cells, MoDCs were isolated from the apoptotic cells using Ficol Paque. Purity of these isolated MoDCs reached over 98%, judged by 5(6)-Carboxyfluorescein diacetate N-succinimidyl ester labeled MoDCs (data not shown). CD86 of the maturation markers on MoDCs (Fig. 5C) was especially more expressed on these cells by HCV-infected apoptotic cells than by noninfected apoptotic cells. HCV-infected apoptotic cells slightly enhanced the expression levels of major histocompatibility complex class I, class II, and human leukocyte antigen-E on MoDCs (data not shown). MoDCs also acquired the increased ability to stimulate allogeneic PBMCs, $CD4^+$ T cells, and $CD8^+$ T cells in response to HCV-infected apoptotic cells (Figs. 5D and 6A).

We determined the ability of $CD4^+$ T cells to produce IFN-gamma (a Th1 cytokine) and IL-4 (a T helper 2 cytokine) after coculture of allogeneic $CD4^+$ T cells and MoDCs exposed to HCV-infected apoptotic cells. These $CD4^+$ T cells produced higher levels of IFN-gamma and lower levels of IL-4 (Fig. 6B) compared to the noninfected control, suggesting that HCV-infected apoptotic cells modulate MoDC func-

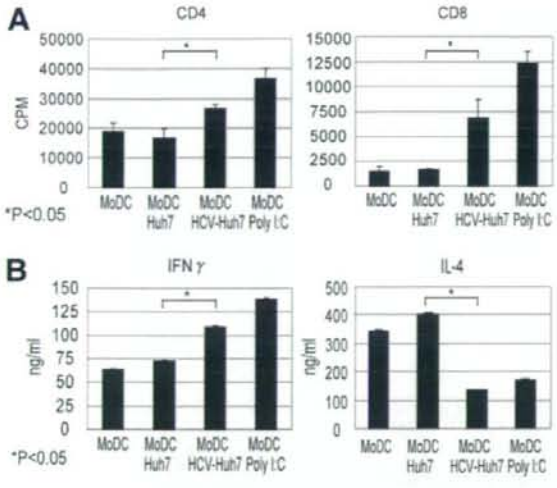

Fig. 6. HCV-infected apoptotic cells modulate MoDC function to polarize the Th1 shift. (A) After 2 days culture with HCV-infected and noninfected apoptotic cells, the isolated MoDCs (1×10^4) were cultured with allogeneic $CD4^+$T cells and $CD8^+$ T cells (1×10^5) for 6 days. Proliferation was determined by $[^3H]$thymidine uptake. (B) Allogeneic $CD4^+$ T cells were harvested after 6 days culture with the MoDCs and stimulated with phorbol 12-myristate 13-acetate and ionomycin for 24 hours. The supernatants were collected to assess the levels of IFN-gamma and IL-4 by ELISA. Poly I:C stimulation was used as a positive control. Data shown are means ± SD of duplicate or triplicate samples from one experiment representative of three donors.

tion to promote Th1-dominant immunity in the Th1/T helper 2 balance.

HCV-Infected Apoptotic Cells Stimulate MoDCs To Activate NK Cells. We next evaluated whether these mature MoDCs could enhance NK activity via MoDC-NK interaction. After exposure of MoDCs to HCV-infected or noninfected apoptotic cells, MoDCs were isolated as described above. HCV-infected apoptotic cells promoted MoDC function to augment NK cell cytotoxicity but not IFN-gamma production compared to noninfected cells (Fig. 7A,B). This up-regulation of NK cell cytotoxicity through MoDC-NK interaction was canceled by separating MoDCs from NK cells with a transwell insertion (Fig. 7C). This suggested that cell-cell contact was the key factor for MoDC-mediated NK cell cytotoxicity induced by coculture with HCV-infected apoptotic cells.

MoDC Maturation Relied on TLR3 Signal Evoked by dsRNA in Apoptotic Vesicles. We surveyed the mechanism of MoDC maturation by HCV-infected apoptotic cells. Since HCV is a positive single-strand RNA virus, dsRNA was detected in HCV-containing apoptotic vesicles by mAb against dsRNA (Fig. 8A). To investigate whether MoDCs were taking up these apoptotic vesicles, we labeled HCV-infected apoptotic cells with the far red fluorescent dye, SNARF-1. MoDCs phagocytosed the SNARF-1-labeled vesicles containing dsRNA, which partially colocalized with TLR3 (Fig. 8B,C). N-[1-(2,3-Dioleoyloxy)propyl]-N, N, N-trimethylammonium methylsulfate (DOTAP)-based transfection was employed for the targeting of RNA to the TLR3-containing endosome.[23] HCV-derived RNA allowed MoDCs to induce IL-6 production as in control poly I:C (Fig. 8D). IL-6 of

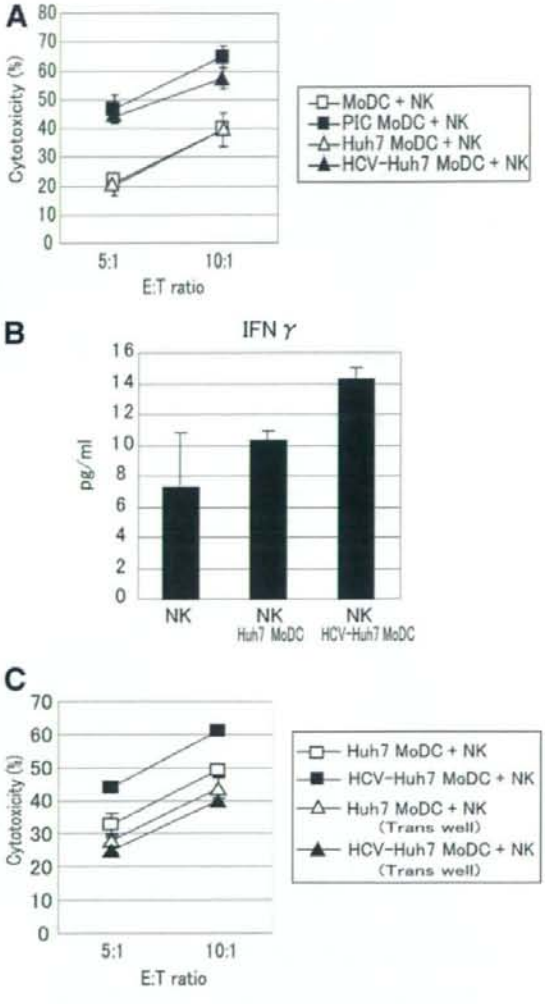

Fig. 7. NK cell activation by MoDCs exposed to HCV-infected apoptotic cells. After 2 days culture with HCV-infected and noninfected apoptotic cells, the isolated MoDCs were cultured with autologous NK cells for 24 hours. (A) NK cytotoxic activity against K562 was determined by ^{51}Cr release assay. Poly I:C stimulation was used as positive control. (B) Supernatant of the MoDC-NK coculture was assayed for NK cell IFN-gamma production. In some experiments, transwell was used to block MoDC-NK cell contact. (C) Using these NK cells, cytotoxic activity was measured by ^{51}Cr release assay. Data shown are means ± SD of duplicate or triplicate samples from one experiment representative of three donors.